NEW TECHNOLOGIES FOR S-BAND AND C-BAND RF STRUCTURE REALIZATION AND THEIR APPLICATION TO THE HIGH GRADIENT/HIGH REPETITION MULTI-BUNCH LINAC FOR THE ELI-NP GAMMA BEAM SYSTEM

David Alesini
(LNF-INFN, Frascati, Italy)

LAL, Orsay, 24 May 2016

OUTLINE

1. **Motivation** for R&D activities in the framework of the ELI-NP project

2. **Damped TW C-band structures** design, fabrication low and high power tests

3. **RF guns** design, fabrication and tests using the new **gasket clamped technique**

4. What next…

MOTIVATION FOR ACCELERATING STRUCTURES CHALLENGES

In the framework of the **ELI-NP** project came out the necessity to develop a **room temperature LINAC** with the following characteristics:

- **Compact** → *High gradient*, *high frequency*
- High brightness → *Photo-injector based*
- **Multi-bunch** → *Damping HOM*, *long RF pulses*, *high dissipated power*
- with a relatively high repetition rate (**100 Hz**) → *high dissipation*
- **Reliable** and as simple as possible in its realization to **reduce costs** and delivery time → *Simplify the mechanics*, *State of the art klystron tech.*, *avoid brazing procedures*

In the framework of high brightness LINACs (SPARC @ LNF and ELI-NP) came out the necessity to develop an **RF photo-GUN** with the following characteristics:

- **Reliable** and as simple as possible in its realization to **reduce costs** and delivery time
- Able to sustain cathode peak field **≥120 MV/m at 100 Hz for Multi-bunches** (long RF pulses) → *Hard copper not brazed*, *high dissipated power*

DAMPED C-BAND STRUCTURES

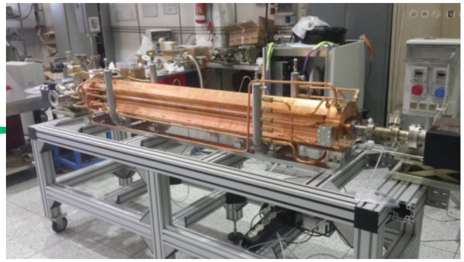

RF GUN CLAMPED

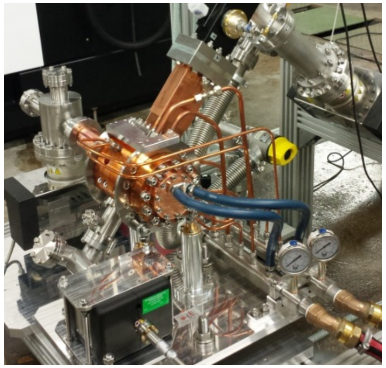

ELI-NP GAMMA BEAM SYSTEM

An advanced **Source of Gamma-ray photons** will be built in Magurele (Bucharest, **Romania**) in the context of the **ELI-NP** Research Infrastructure by the "EuroGammaS" Association. The photons will be generated by **Compton back-scattering** in the collision between a high quality electron beam and a high power laser. The machine is expected to achieve an energy of the gamma photons tunable between 1 and 20 MeV with a narrow bandwidth (0.3%) and a high spectral density (10^4 photons/sec/eV). The machine is based on a RF Linac operated at C-band (5.712 GHz) with an S-band photoinjector delivering a high phase space density electron beam in the **300-740 MeV energy range**. The repetition rate of the machine is **100 Hz** and, within the RF pulse, up to **32 electron bunches** will be accelerated, each one carrying **250 pC** of charge, separated by **16 ns**. The linac booster is composed of **12 TW C-Band** disk loaded accelerating structures, each structure, 1.8 m long, is a quasi-constant gradient structure with 2π/3 field phase advance per cell.

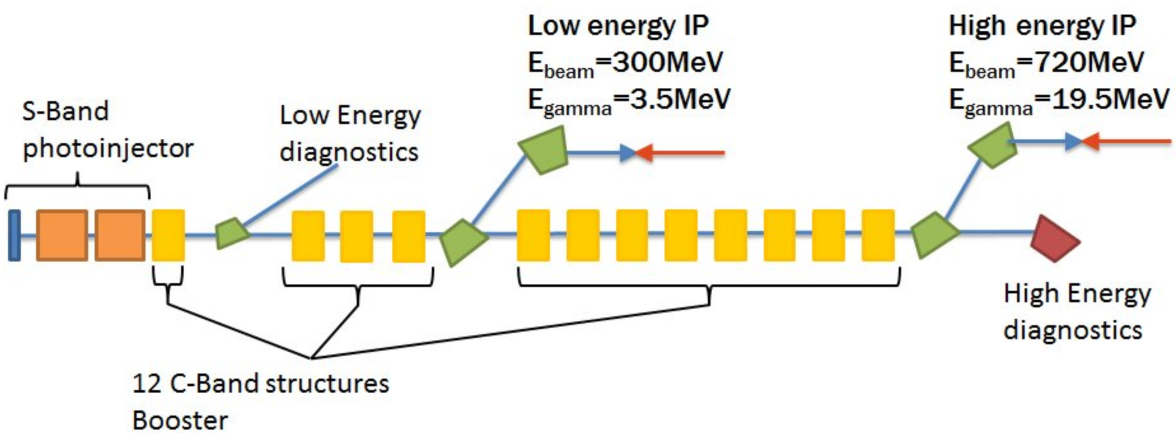

Bunch charge	250 pC
Number of bunches	32
Bunch distance	16 ns
C-band average accelerating gradient	33 MV/m
Norm. emittance	0.4 mm·mrad
Bunch length	<300 μm
RF rep Rate	100 Hz

European Collaboration for the proposal of a Gamma-Beam System to the ELI-NP Project

The **"EuroGammaS" Association** is composed by the INFN, the "Association leader", the University of Rome "La Sapienza", the CNRS, ACP S.A.S., Alsyom S.A.S., Comeb Srl, ScandiNova Systems AB.

ACCELERATING STRUCTURES FOR ELI-NP GBS

1 S Band gun

2 TW S Band accelerating structures SLAC-type

12 TW C-band damped accelerating structures

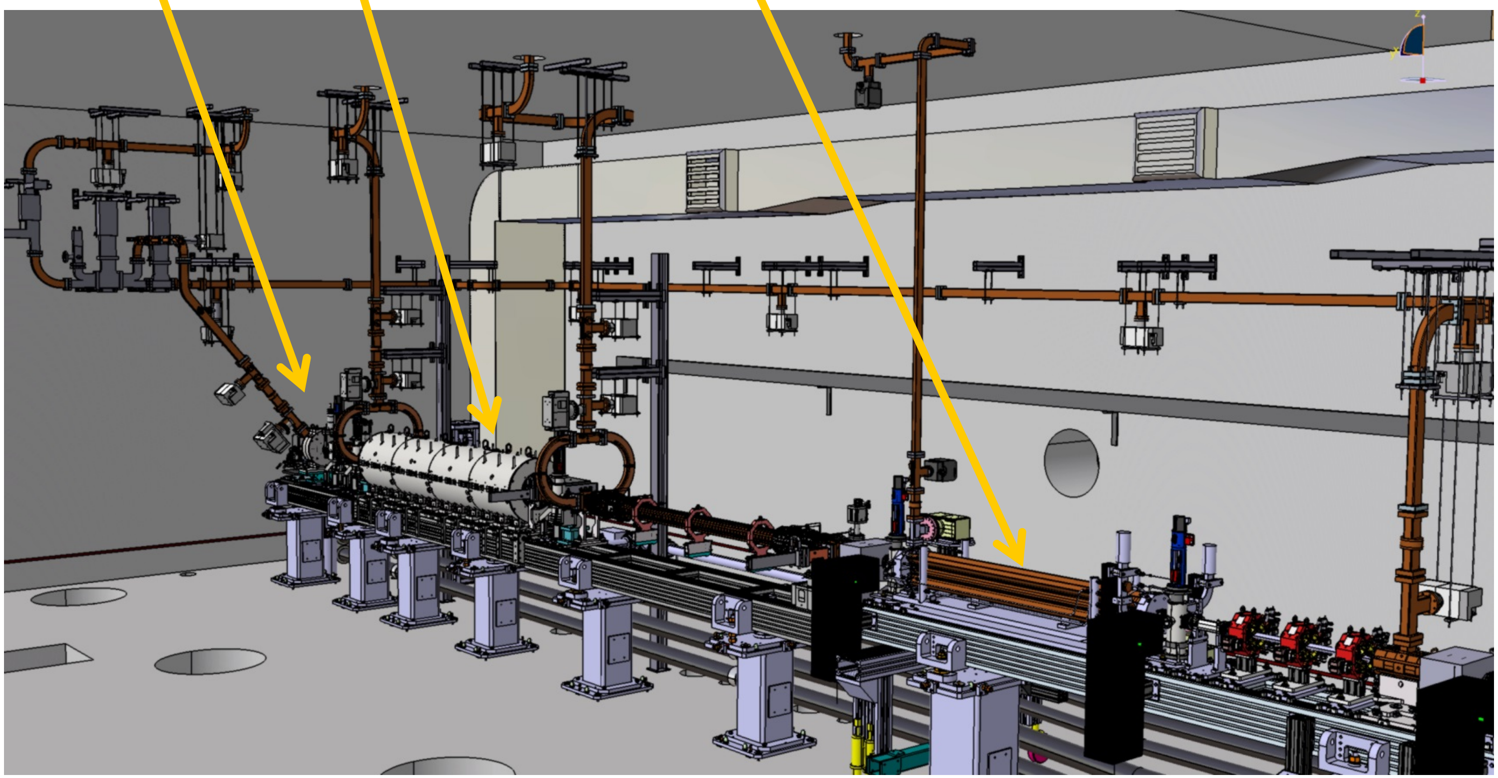

C-BAND STRUCTURES

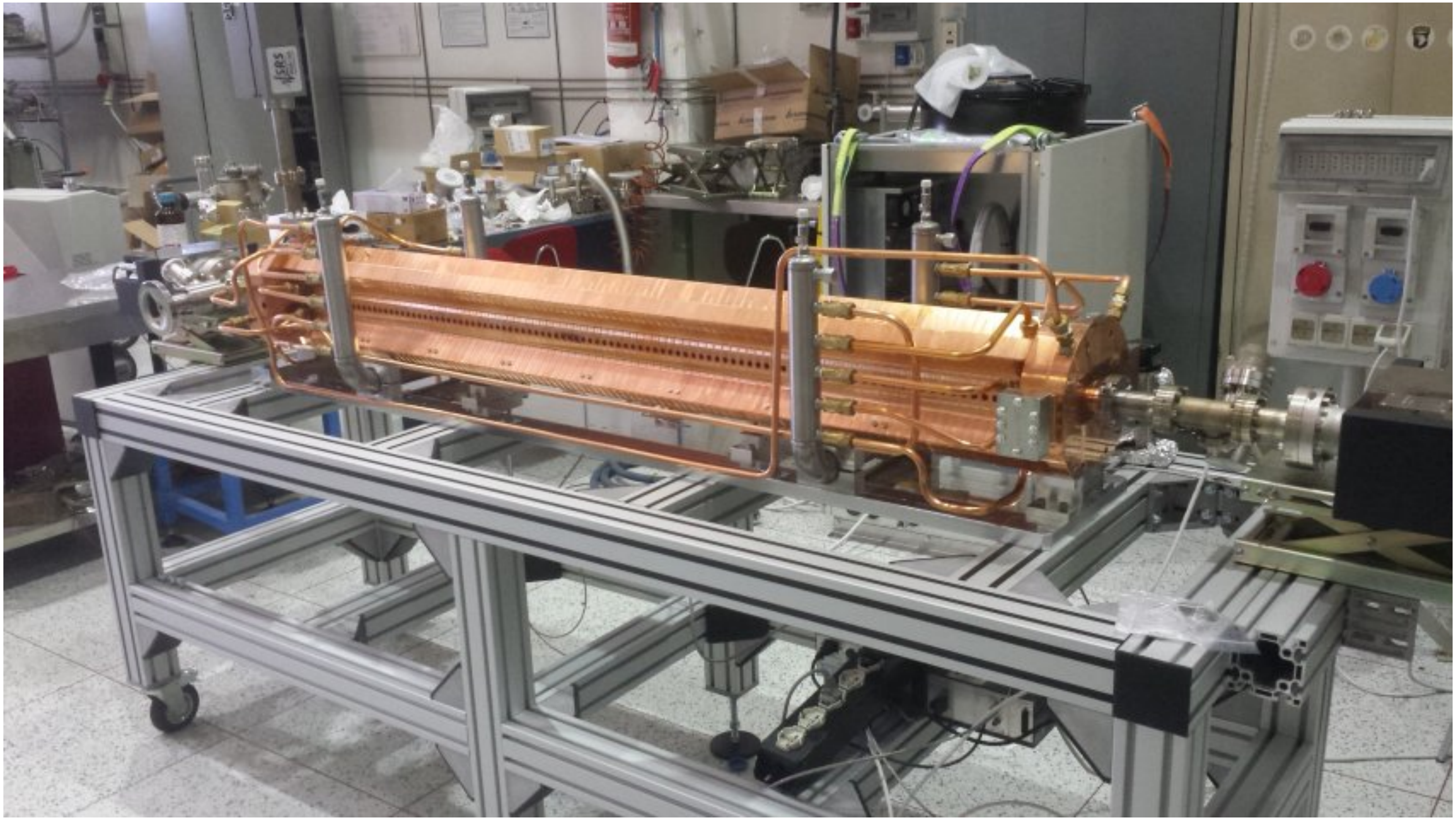

ACCELERATING STRUCTURES CHALLENGES IN ELI-NP GBS

To increase the gamma flux we need to **increase the number of collision per second** → **100 Hz** repetition rate; **Multi bunch**

- **-Damping of HOM** in RF structures to avoid BBU instabilities
- -Compensation of **beam loading effects**
- **-accurate thermal design (high average dissipate power)**

To reduce the accelerator overall dimensions: **compact system** → **High gradient**

-C-band LINAC combined with an S-band Injector is the best compromise between BD and compactness of the system

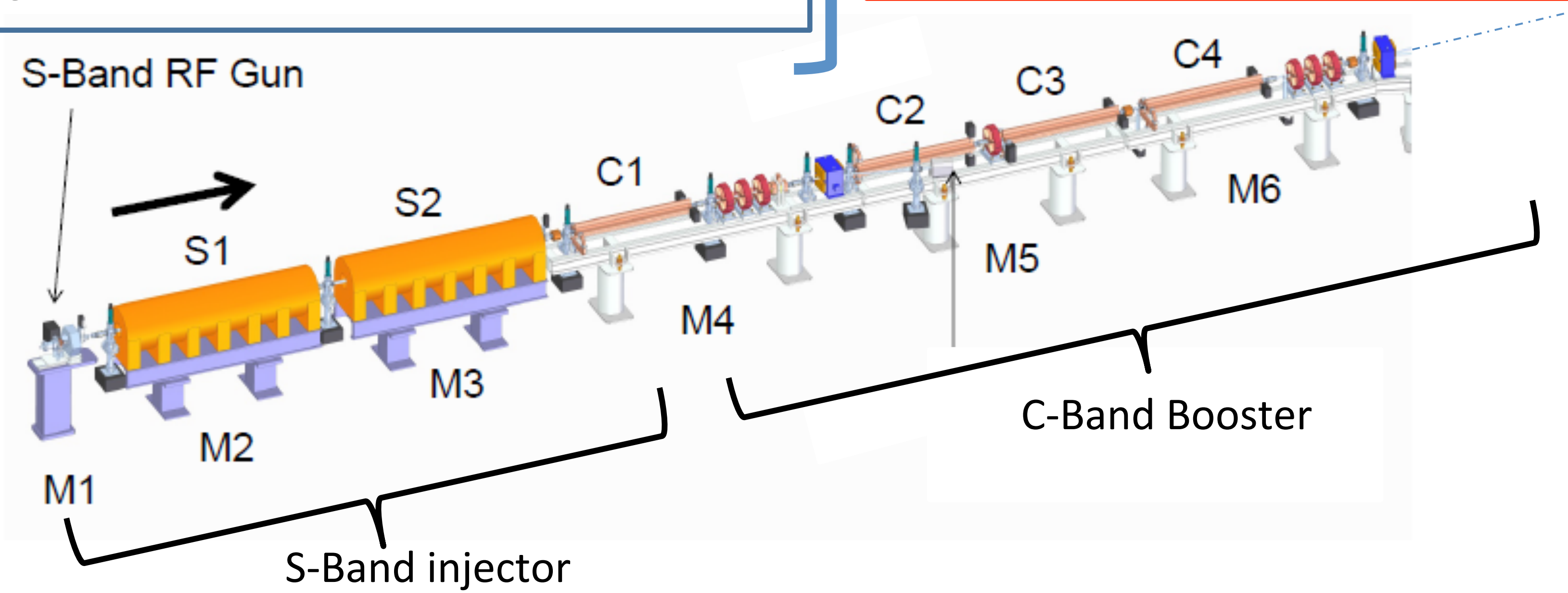

BEAM BREAK-UP WITH C-BAND CAVITIES

The **ELI-NP GBS LINAC operates in multi-bunch mode**. The passage of electron bunches through accelerating structures excites electromagnetic **wakefield**. This field can have longitudinal and transverse components and, interacting with subsequent bunches, **can affect the longitudinal and the transverse beam dynamics**. Those related to the excitation of the fundamental accelerating mode are referred as **beam loading effects** and can give a modulation of the beam energy along the train while **transverse wakefields**, can drive an instability along the train called **multibunch beam break up** (BBU)..

TRANSVERSE EFFECTS $\Rightarrow$ Cumulative beam break-up (BBU)

LONGITUDINAL EFFECTS $\Rightarrow$ beam loading

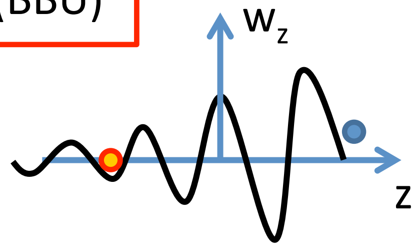

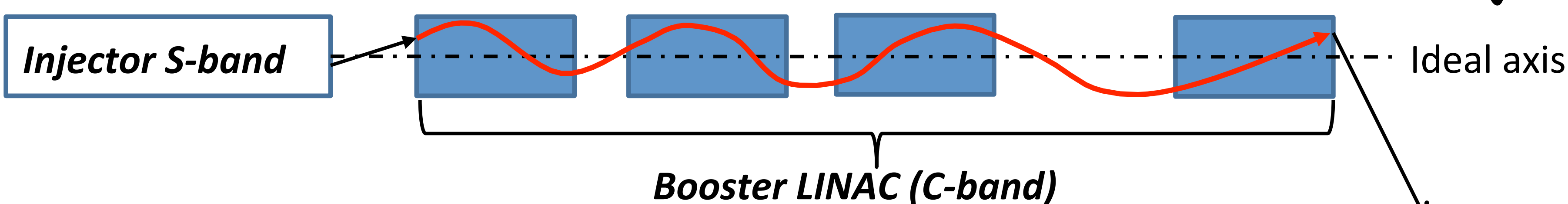

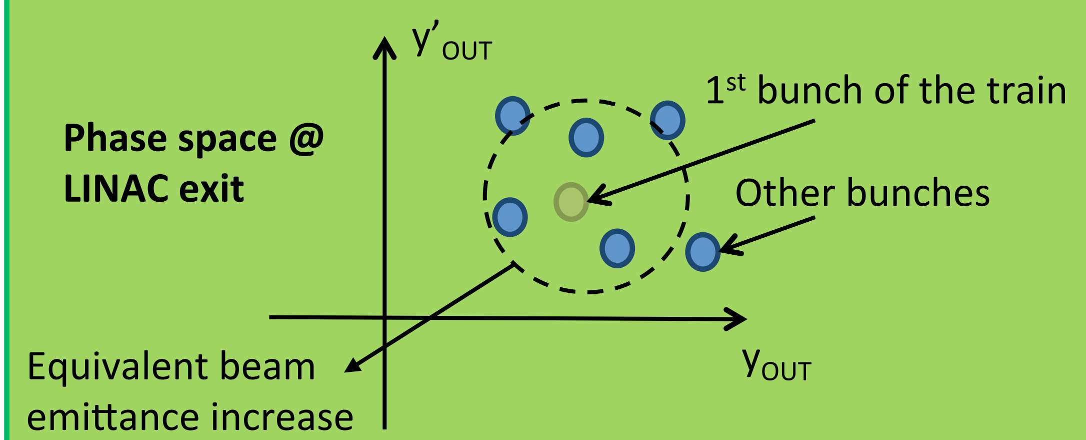

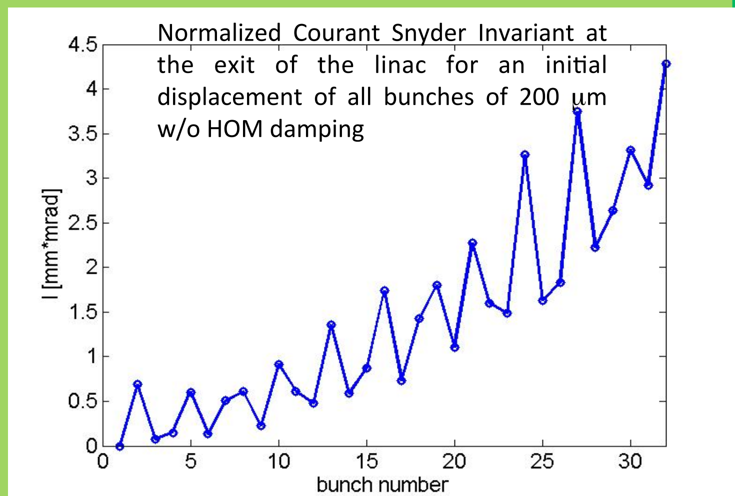

DAMPING OF DIPOLE MODES CHOICE

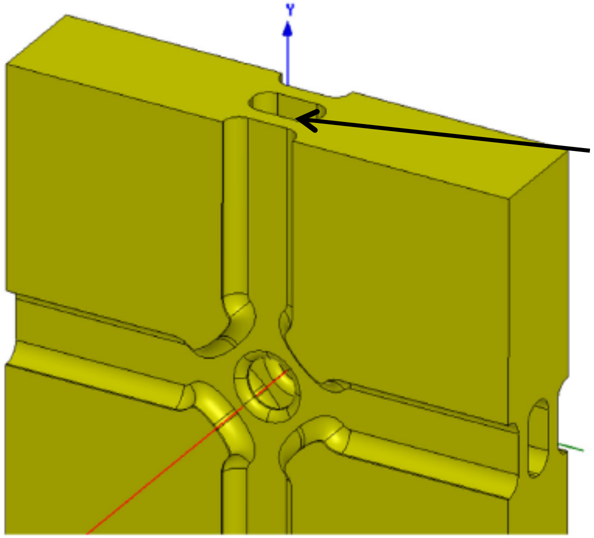

Dipoles modes propagate in the waveguide and dissipate into a RF loads

CLIC structures X-band, high gradient

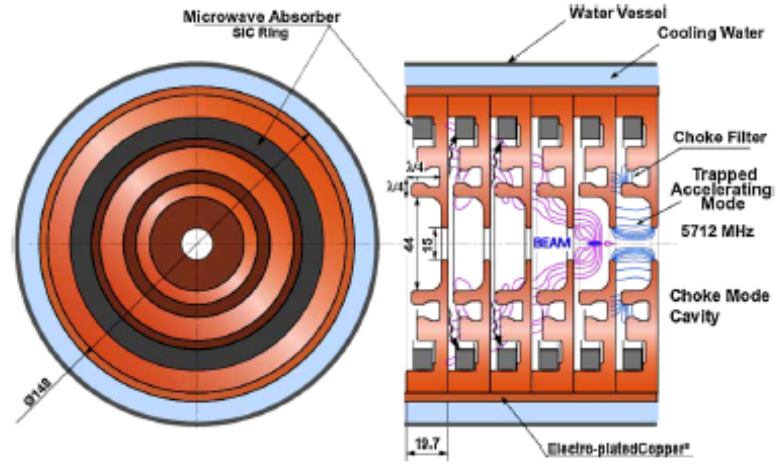

C-Band structures Spring-8

Advantages

1. Strong damping of all modes above waveguide cut-off
2. Possibility of tuning the cells
3. Good cell cooling (100 Hz, multi-bunch)
4. Higher shunt impedance

Disadvantages

1. Machining: need a 3D milling machine
2. Multipole field components (octupole) but not critical for BD

Advantages

1. Easy machining of cells (lathe)
2. 2D geometry: no multipole field components

Disadvantages

1. Critical e.m. design: notch filter can reflect also other modes.
2. Not possible to tune the structure
4. Cooling at 100 Hz, long pulse length (?)

C-BAND STRUCTURES DESIGN: HOM SUPPRESSION

Since the ELI-NP linac operation is **multi-bunch**, in order to achieve the requested photon flux, the structures have been designed with an effective **damping of the HOM dipoles** modes to avoid BBU instabilities. The solution adopted for the ELI-NP structures is based on a **waveguide damping system**. Each cell of the structure has four waveguides that allows the excited HOMs to propagate and dissipate into silicon-carbide (SiC) RF loads. Electromagnetic simulations have been done using the frequency domain code **HFSS** and the time domain code **GdFidL and CST** to design the cells and to optimize the waveguide coupling apertures.

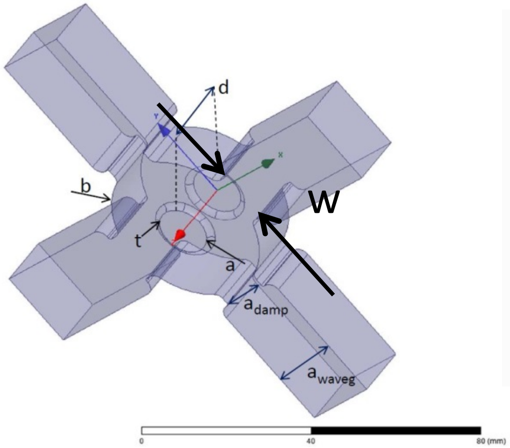

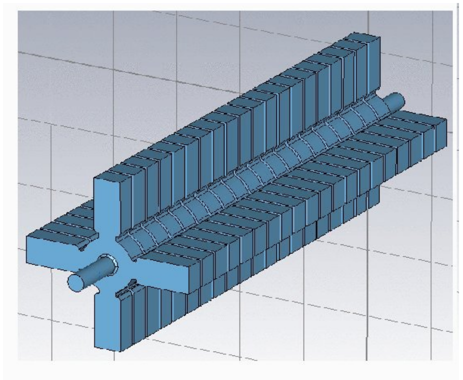

(a)

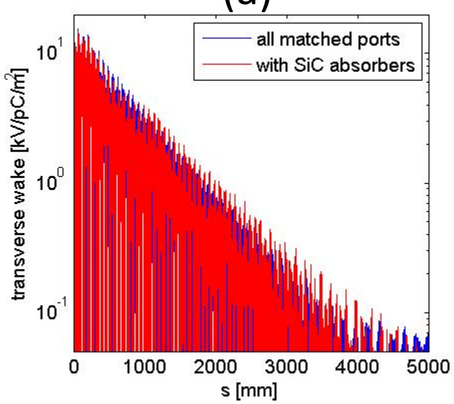

(b)

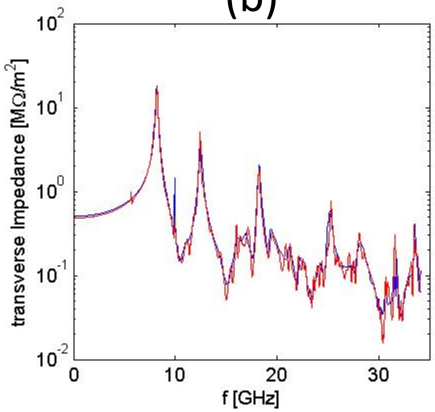

(a) transverse wakepotential per unit length calculated by CST: beam sigma 3mm, beam off axis 2 mm; (b) corresponding transverse impedance.

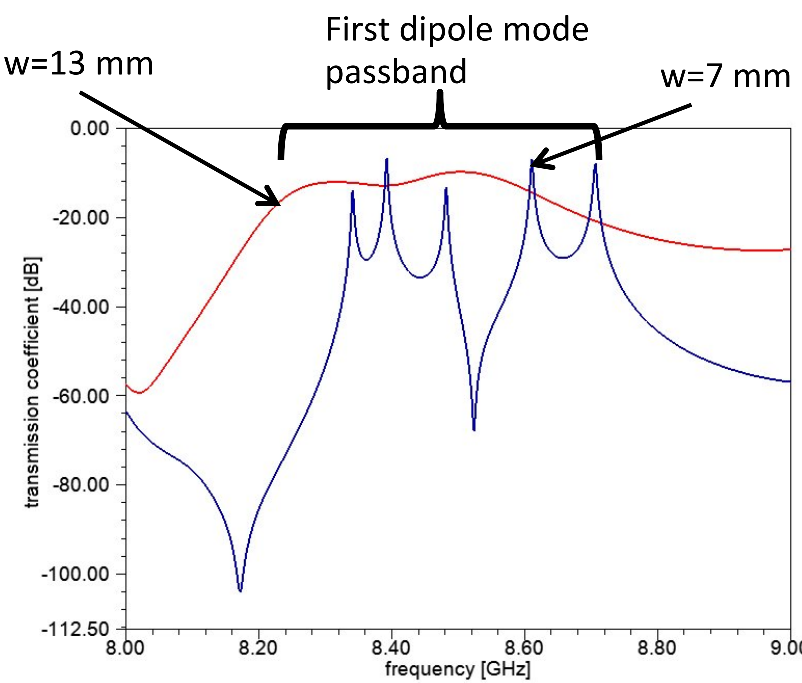

[D. Alesini et al., WEPFI013, Proceedings of IPAC2013, p. 2726]

C-BAND STRUCTURES DESIGN: QUASI CONSTANT GRADIENT

Each structure is fed by a **single klystron with a constant RF input pulse** (40 MW) and the apertures of the irises have been shaped to have a **quasi-constant accelerating field** (from 38 to 28 MV/m). It has been decided to adopt such a design with respect to a constant impedance structure because, in this last case, to achieve an **average accelerating field of 33 MV/m**, the accelerating field in the first cell has to be increased to more than 44 MV/m, giving potential problems from the breakdown rate point of view. On the other hand a perfect constant gradient structure requires very small irises at the end of the structure with a consequent increase of the dipole mode effectiveness, reduction of the pumping speed and beam clearance. The final profile of the accelerating field on axis is given in the figure.

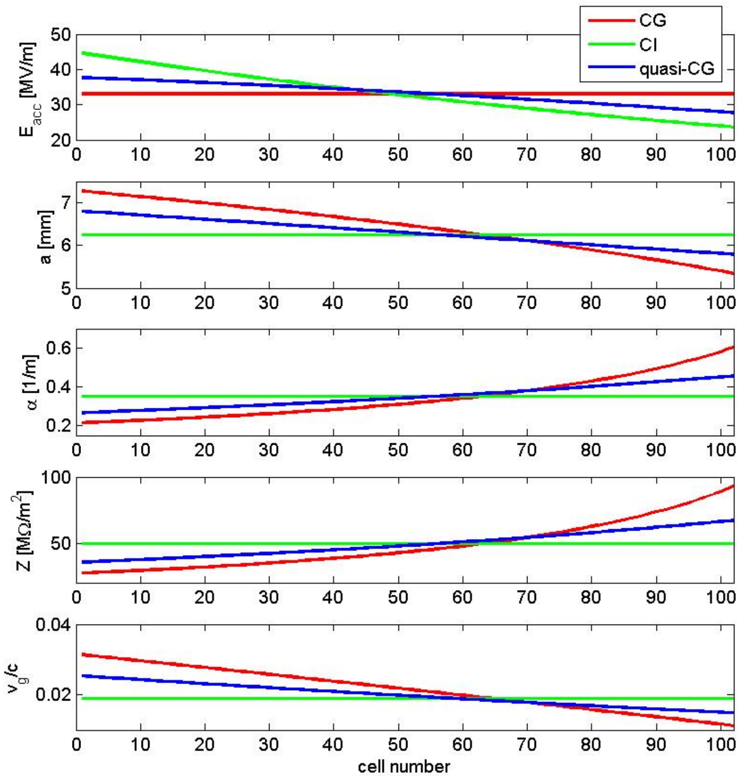

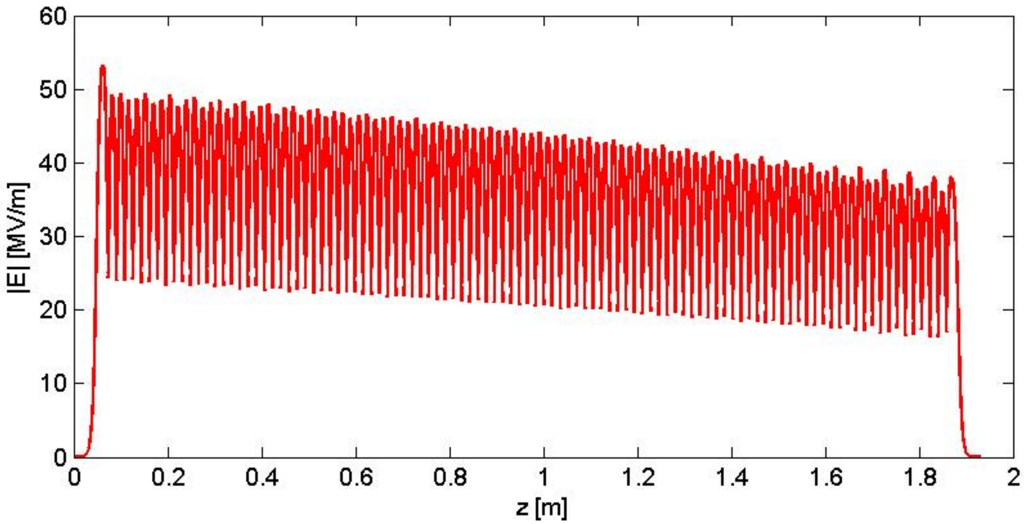

HFSS simulations

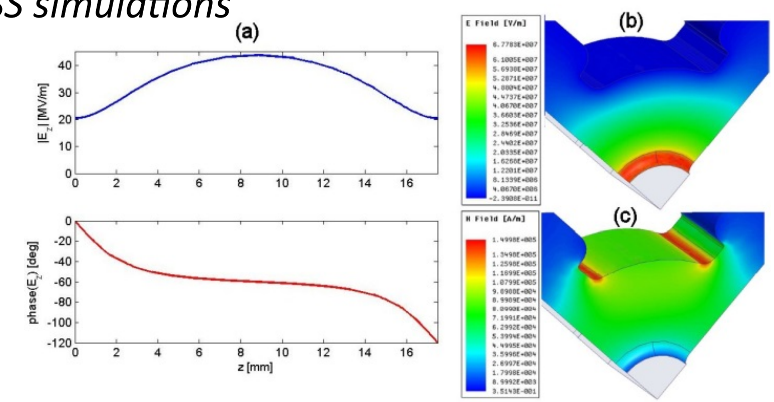

[D. Alesini et al., THPRI042*, Proceedings of IPAC2014, p. 3856]*

C-BAND STRUCTURES DESIGN: COUPLERS

The **input and output couplers have a symmetric feeding and rounded edges** to reduce the pulsed heating on the surfaces. The **input coupler integrates a splitter** to allow symmetric RF feeding while the output one has two symmetric outputs connected to two RF load. The couplers have been designed with a **race-track shape to completely suppress the quadrupole field components** induced by the presence of the waveguide hole apertures. In the plot below there are reported the amplitudes of the multipole magnetic field components in the center of the coupler cells as a function of the race-track thickness. The final coupler race track dimensions have been chosen to completely suppress the quadrupole components in both the input and output couplers: Δx=6.3 mm and Δx=5.2 mm for the input and output coupler respectively.

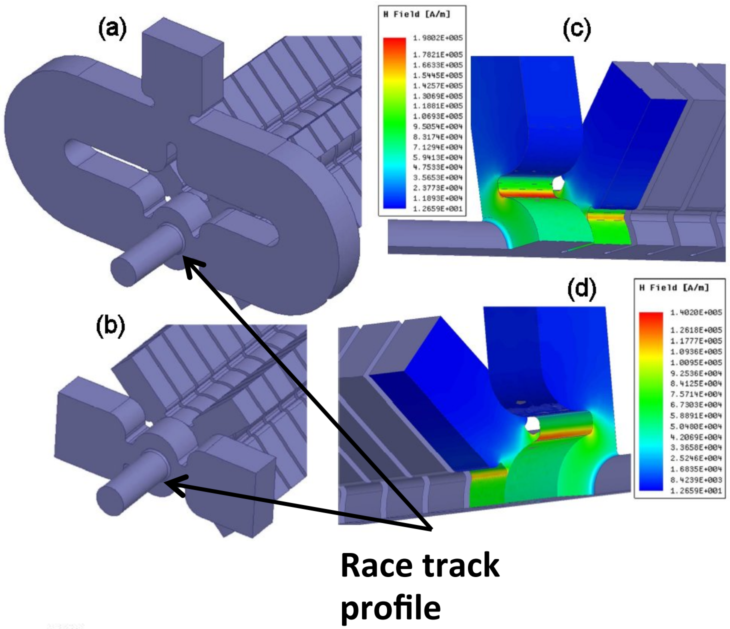

Multipole magnetic field components in the center of the input/output coupler cells.

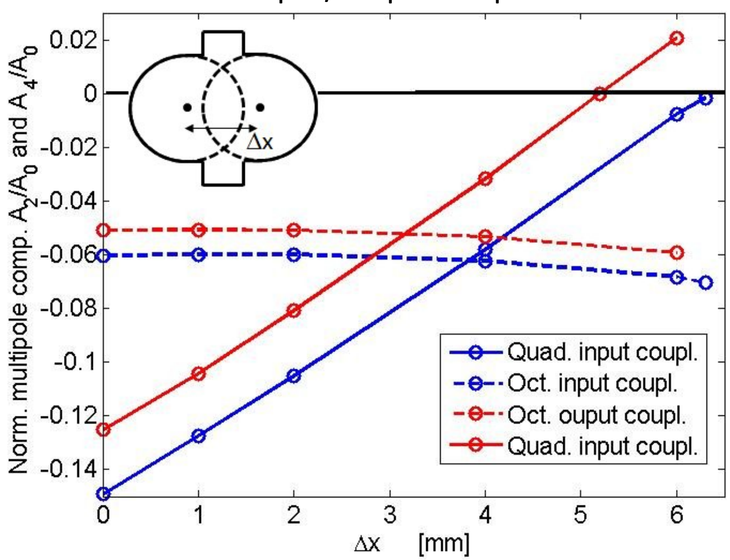

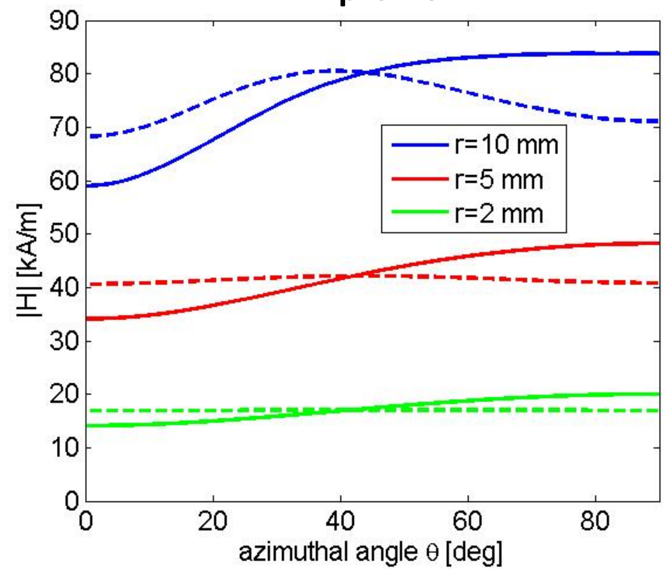

[*D. Alesini et al.*, THPRI042, *Proceedings of IPAC2014, p. 3856,*
D. Alesini et al., NIM A, 580 1176–1183, (2007)*]*

C-BAND STRUCTURES DESIGN: SiC RF ABSORBERS

The **geometry of the SiC absorbers have been strongly simplified** to minimize complications in the fabrication process, thus reducing the overall production cost and the risk of failure. The overall structure has been conceived in **modules, each of 12 cells** with four SiC long tiles absorbers. Each 12 cell stack is brazed and all stacks are finally assembled and brazed with the input and output couplers. From the electromagnetic point of view the SiC tiles have a very simple geometry that guarantees, at the same time, the RF performances. The optimization of the tile profiles has been done using HFSS. We have chosen the Ekasic-P material for its electrical properties. Time domain simulations with **GdFidL and CST** have been finally done to verify the overall performances.

TIME DOMAIN (CST)

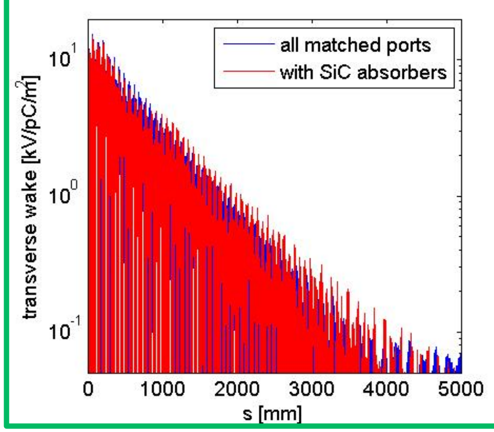

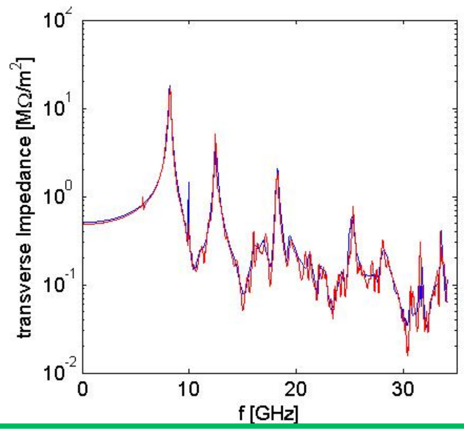

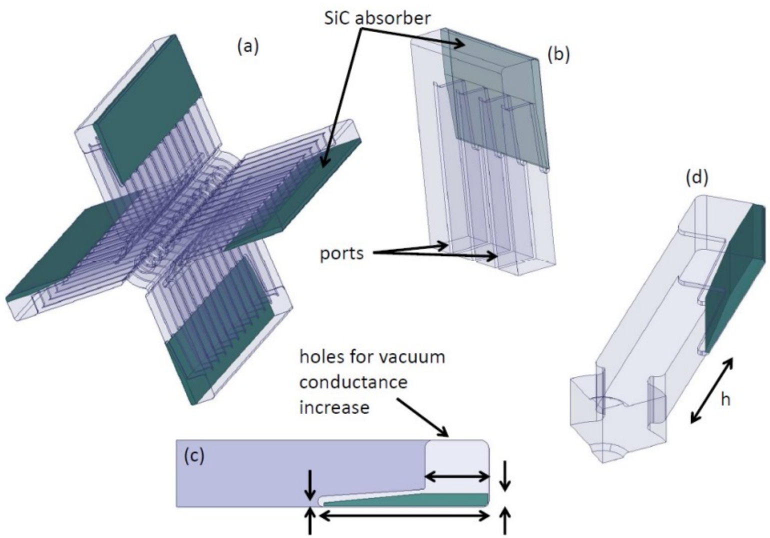

FREQUENCY DOMAIN (HFSS)

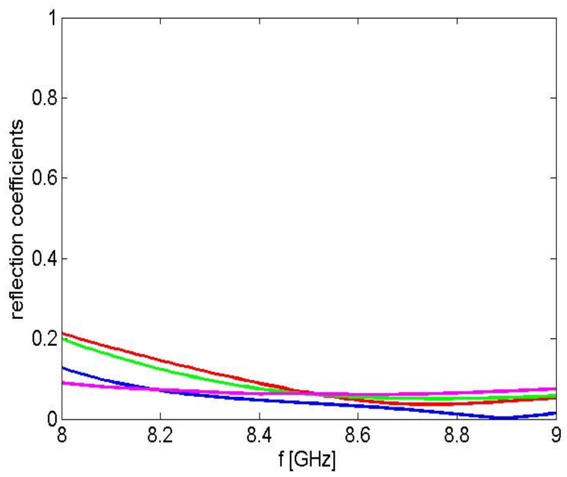

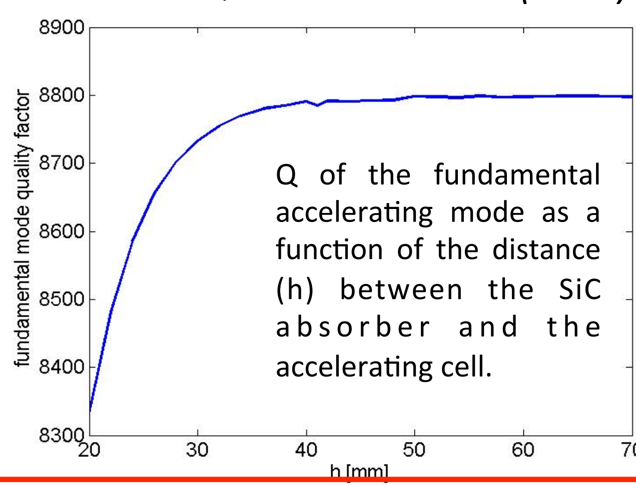

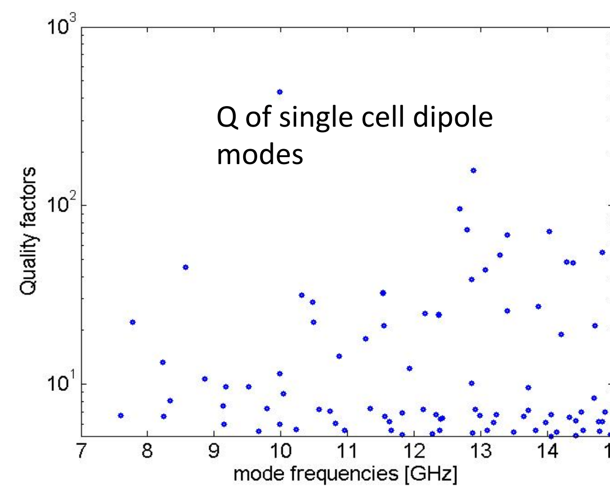

C-BAND STRUCTURES: THERMAL ANALISYS AND VACUUM

A **detailed thermal analysis with ANSYS** has been done to demonstrate the feasibility operation of the structure under the 100 Hz operation with a 2.3 kW average dissipated power. The temperature distribution along the structure is given in the figure and the resulting mechanical deformation does not give significant detuning of the structure. Each structure has 14 cooling channels: 2 for the input coupler, 2 for the output coupler, 8 for the structure and 2 for the output loads. The total water flow is 66 liter/min.

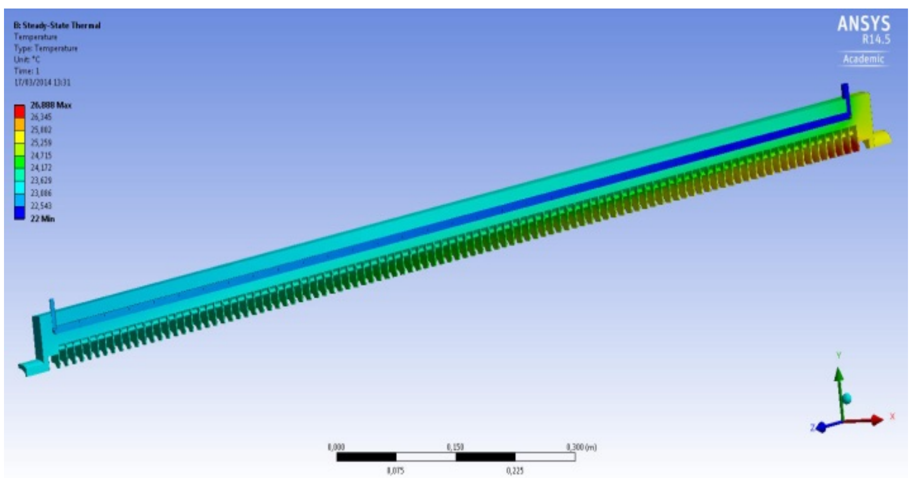

temperature distribution along the C-Band structure (assuming a water temperature of 22 C).

Vacuum calculations have been performed to evaluate the vacuum pressure along the structure. Two pumping units are foreseen in the structure one at the entrance and one at the end. The pressure profile along the axis of the structure is given in the figure for two different values of the specific outgassing rate of the copper and of the SiC absorbers.

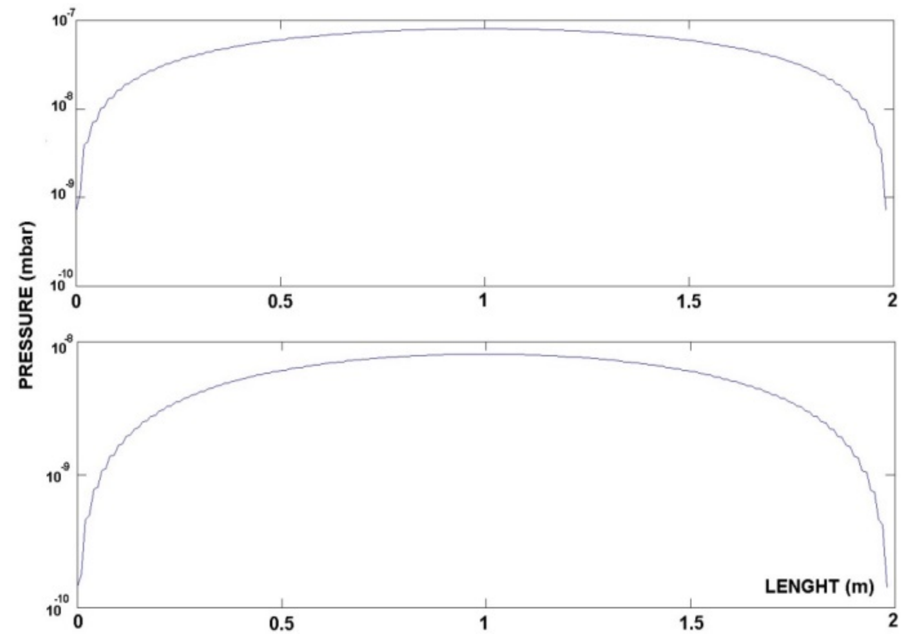

pressure profile along the axis of the structure for two different values of the specific outgassing rate

[V. Pettinacci et al., THPRI043, *Proceedings of IPAC2014, p. 3860]*

[D. Alesini et al., THPRI042, *Proceedings of IPAC2014, p. 3856]*

C-BAND STRUCTURES FINAL PARAMETERS

Structure type	**Quasi-CG**
Working frequency (f_{RF})	5.712 [GHz]
Number of cells	102
Structure length	1.8 m
Working mode	TM_{01}-like
Iris half aperture radius	6.8-5.78 mm
Cell phase advance	$2\pi/3$
RF input power	40 MW
Average accelerating field	33 MV/m
Accelerating field input-output	37-27 MV/m
Average quality factor	8870-8840
Shunt impedance	67-74 MΩ/m
group velocity (v_g/c)	0.025-0.015
Filling time	313 ns
Output power	0.29·Pin
Pulse duration for beam (τ_{BEAM})	<512 ns
Rep. Rate (f_{rep})	100 Hz
Pulsed heating accelerating cells	<8 ^{o}C
Pulsed heating input coupler	<21 ^{o}C
Average dissipated power	2.3 kW
Working temperature	30 °C

C-BAND STRUCTURES: MECHANICAL DESIGN

Each cell of the structure has four waveguides that allows the excited HOMs to propagate and dissipate into silicon-carbide (SiC, EKASIC-P) RF loads. The cells **have four tuners and eight cooling pipes** to sustain the 100 Hz operation. A thorough optimization analysis of the mechanical and electromagnetic design has been carried out to **simplify the mechanical** drawings and the fabrication procedure thus reducing the **overall cost** of production maintaining, at the same time, the structure performances. In particular the **geometry of the SiC absorbers has been strongly simplified** as shown in the figure. In each stack of 12 cells there are four SiC long absorbers, each stack is brazed and all stacks are finally assembled and brazed with the input and output couplers.

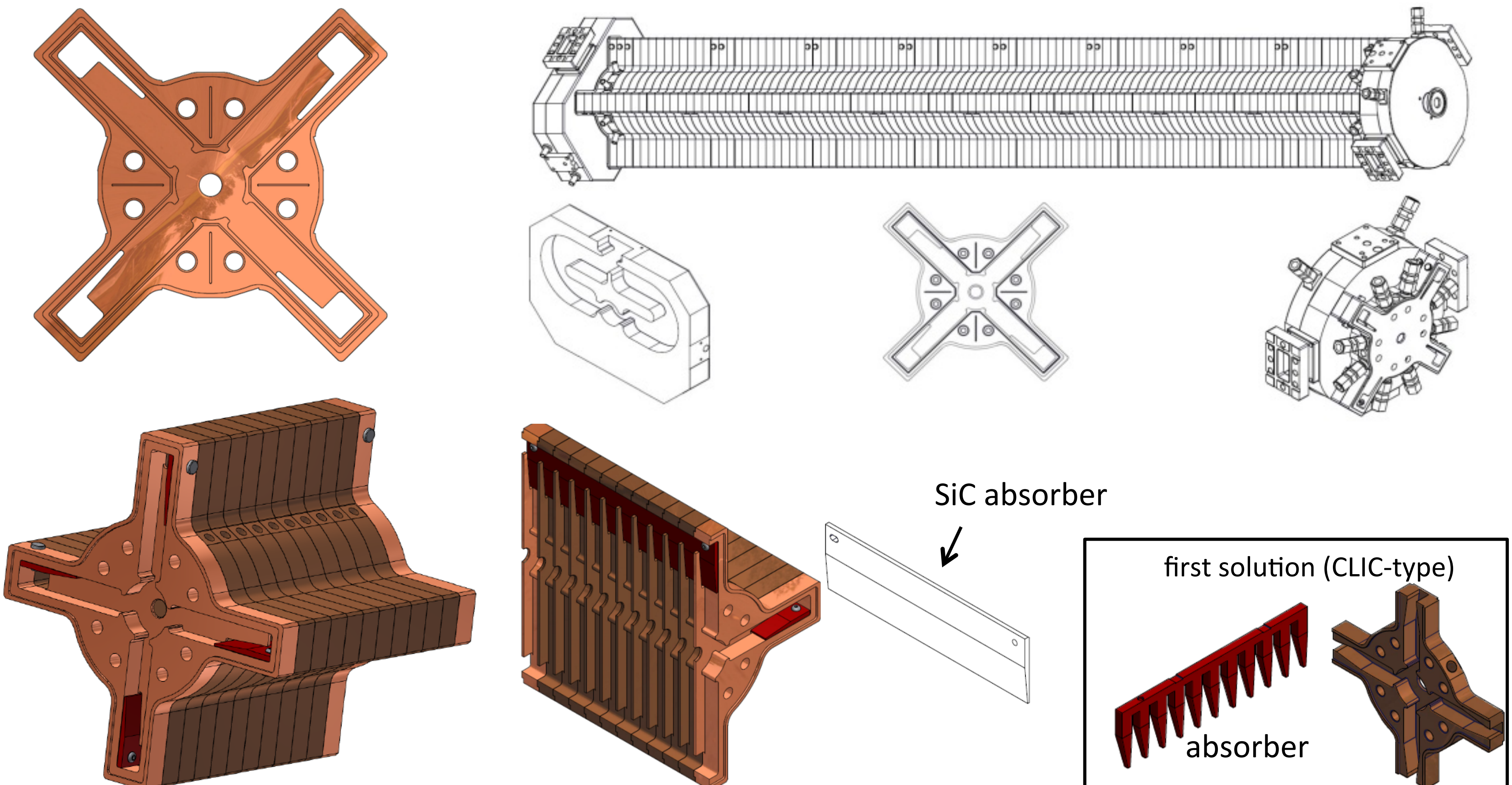

C-BAND STRUCTURES: FABRICATION

The **manufacturing of the cells** required several steps:

1) Rough machining
2) Stress relieving treatment in a vacuum furnace at 500°C for 1 hour
3) Milling of the cell (in particular waveguides apertures and pre-machining of the irises)
4) Ultra-precise manufacturing of irises and cells with lathe (precision ±3 μm and roughness ≤ 50 nm)

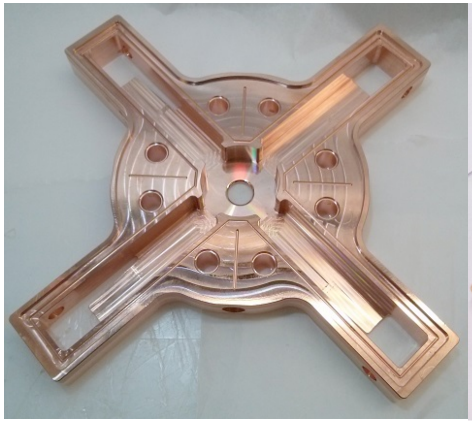

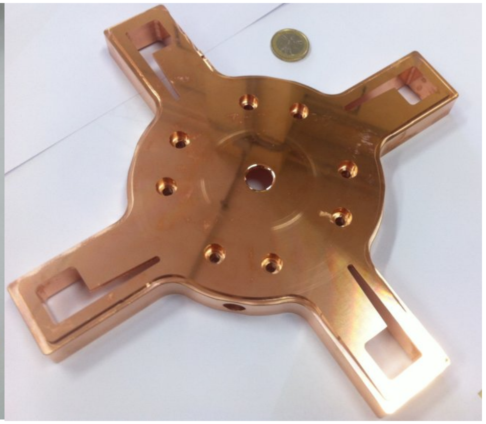

Manufacturing of the **input and output couplers**:

1) Rough machining
2) Stress relieving treatment in a vacuum furnace at 500°C for 1 hour
3) Milling

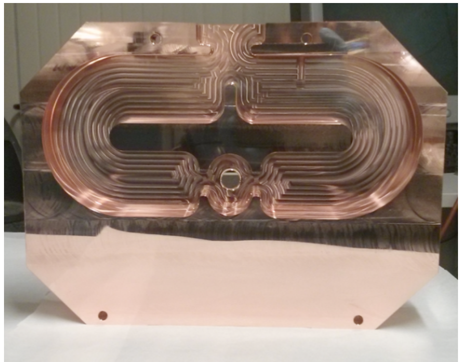

Cleaning of the machined components:

1) Removal of the machining oils with neutral soap
2) Removal of copper oxidations with weak acid (citric)
3) Almeco 19 at 48-50 degree for 5 minutes
4) Rinse with raw water
5) Ultrasound cleaning with NGL at 50 degrees
6) Rinse with raw water
7) Demineralized water in ultrasound at 20 degrees for 10 minutes
8) drying with nitrogen flow
9) packaging

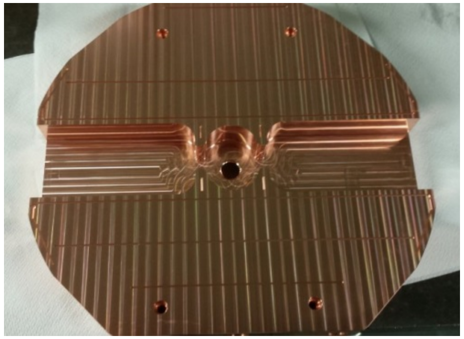

Machining and brazing have been done by Comeb (ELI-NP partner) and in the INFN-LNL oven under LNF supervision

C-BAND STRUCTURES: BRAZING

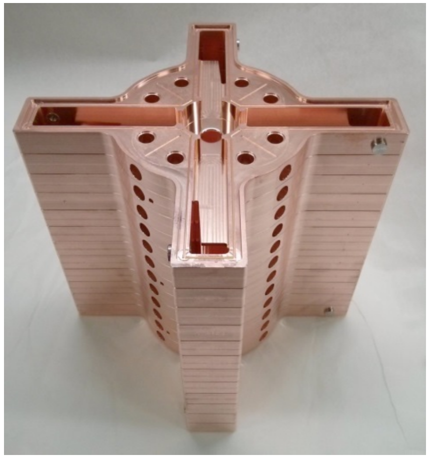

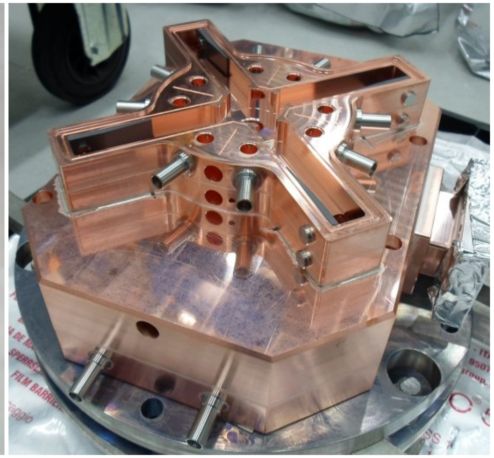

The structure has been brazed in several steps:

1) **Modules of 12 cells** (8 for each structure) and input/output couplers have been brazed with **Palcusil 10** at 850 degrees and vacuum/mechanically tested after brazing.

2) The **SiC absorbers have been inserted** in the cells.

3) **Brazing of two sub-assembly** (6 modules+output coupler and two modules plus the input coupler) with **Palcusil 5** at 810°C.

4) The two sub assemblies have been joined with **Cusil** at 780°C. The last two brazing steps have been performed in the INFN LNL–LEGNARO oven.

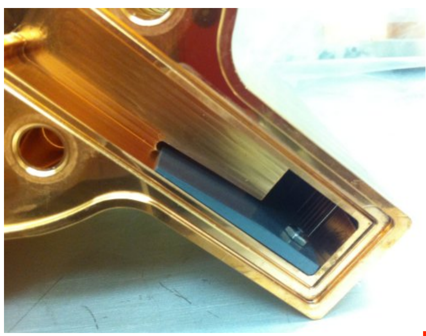

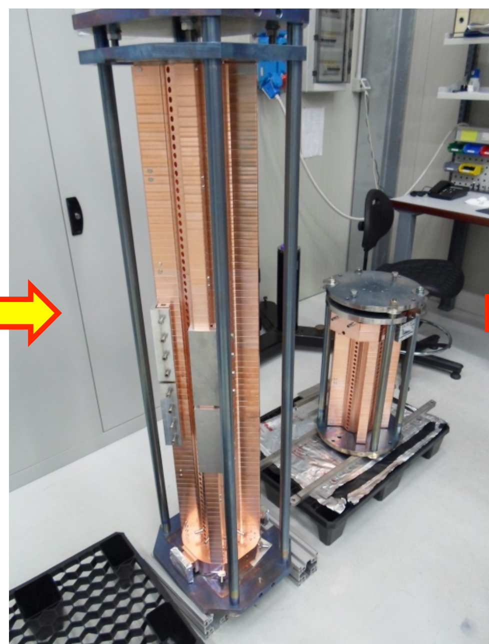

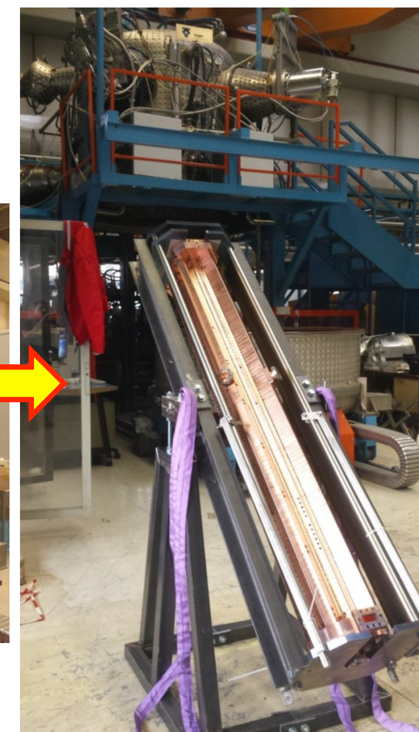

FINAL C-BAND STRUCTURE

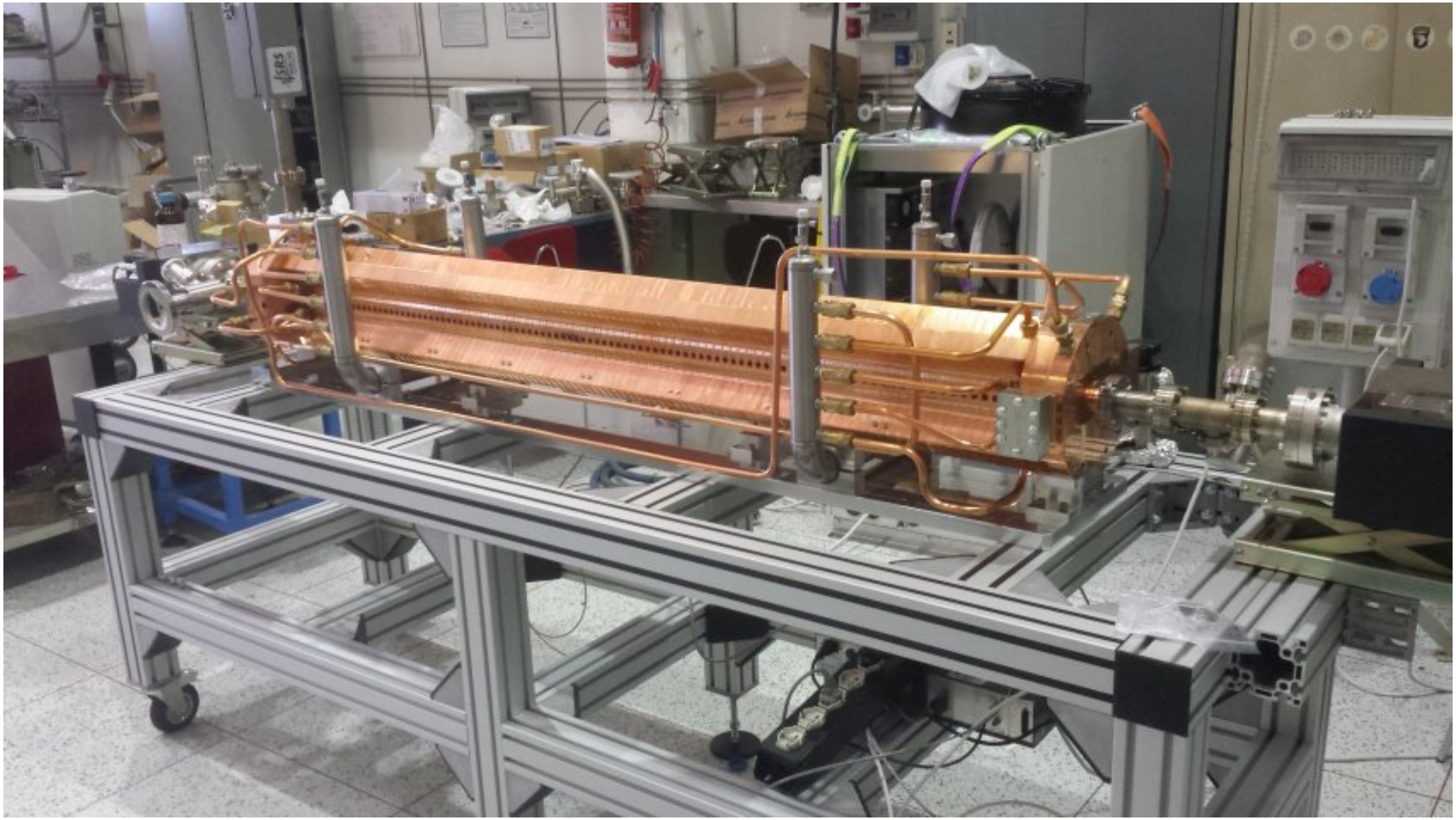

C-BAND STRUCTURES: RF MEASUREMENTS

RF test at low power have been performed in the **single 12 cell module** with and without the SiC absorbers. The transmission coefficient between two antennas coupled with the structure modes have been measured.

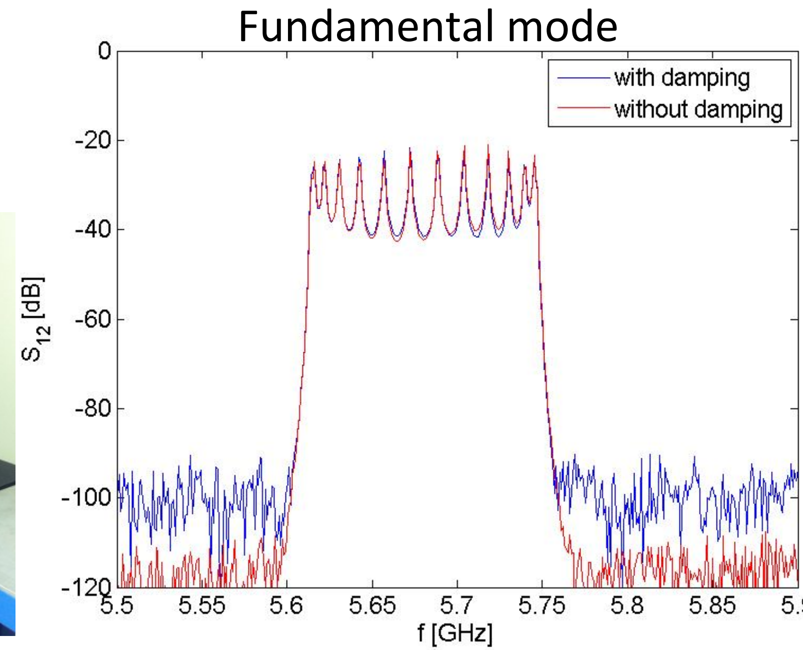

The **measurements show the effectiveness of the SiC absorbers** since the HOM disappear after the insertion of the absorber themselves. The remaining modes are TE-like modes that have a negligible transverse and longitudinal impedance.

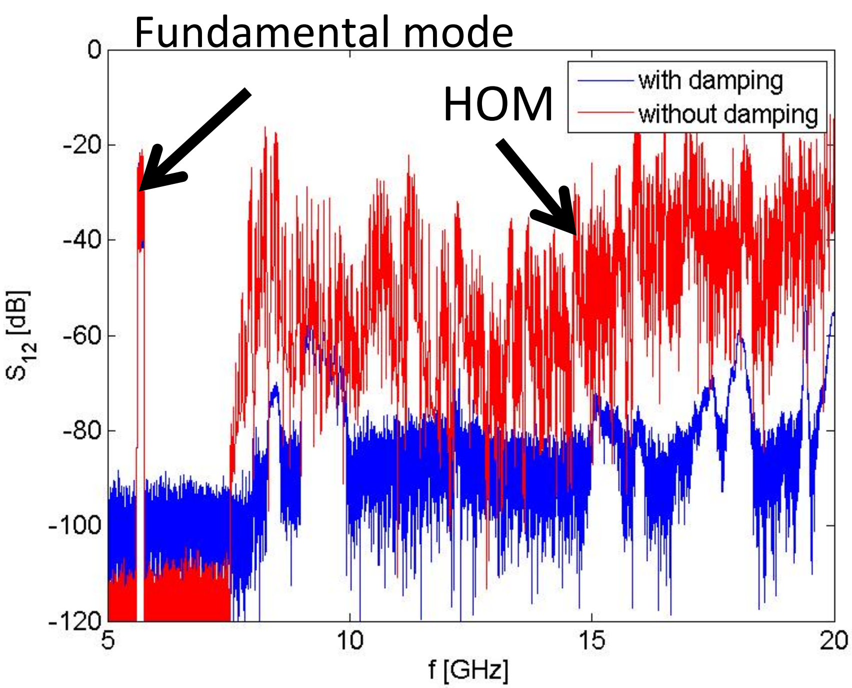

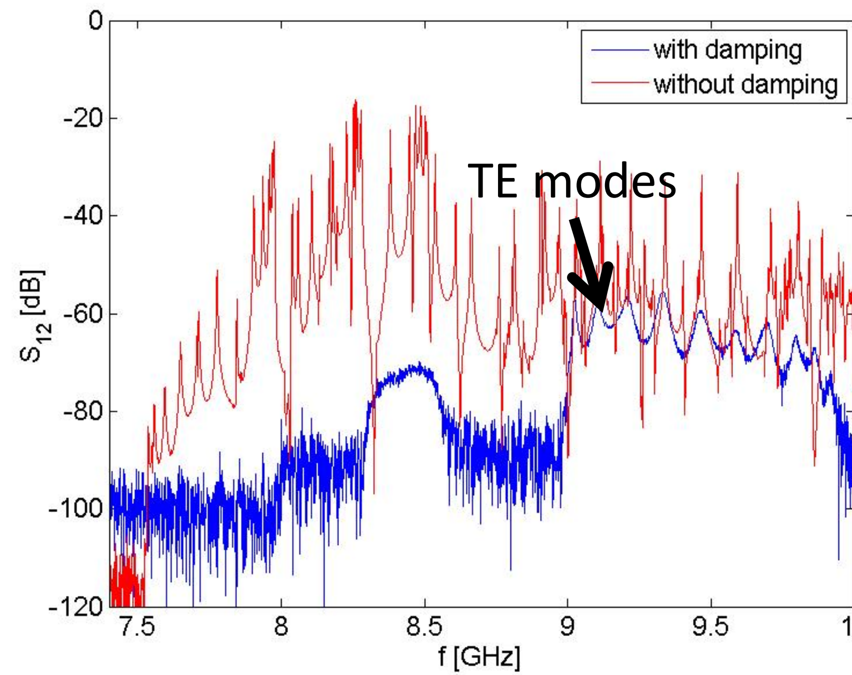

C-BAND STRUCTURES: TUNING

Electric field into the structure has been measured using the **bead pull technique** and the **structure has been tuned** using the local reflection coefficient technique (J. Shi et al., Proc. of LINAC 2010, Tsukuba and D. Alesini, et al., 2013 JINST 8 P10010).

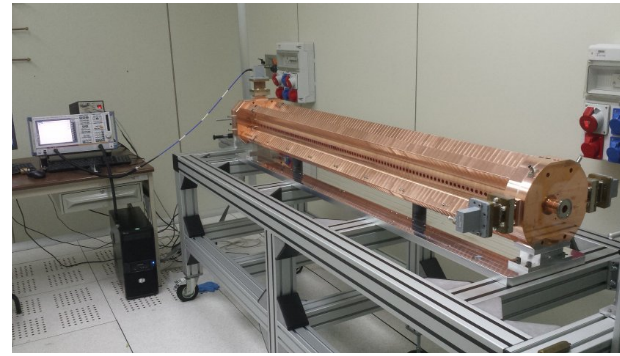

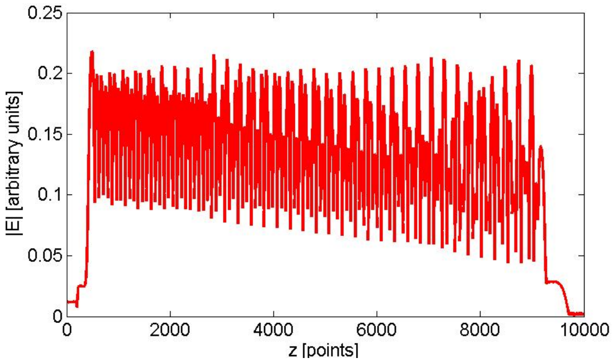

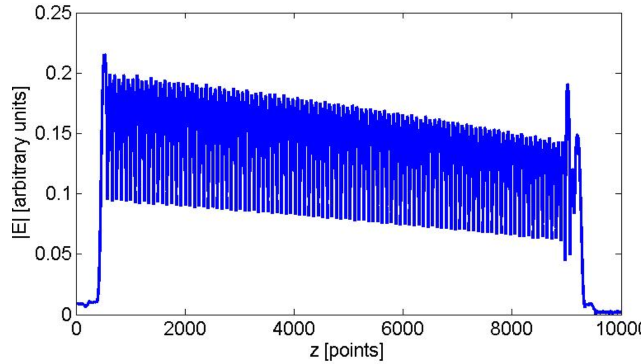

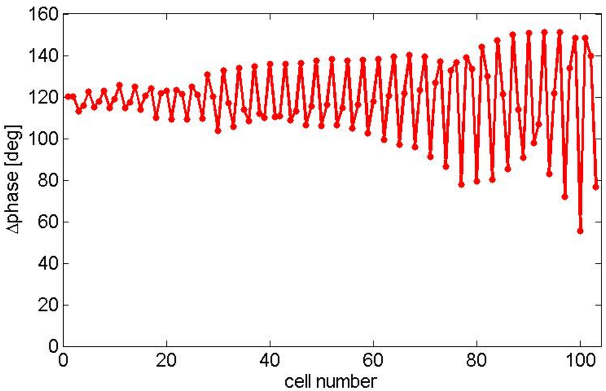

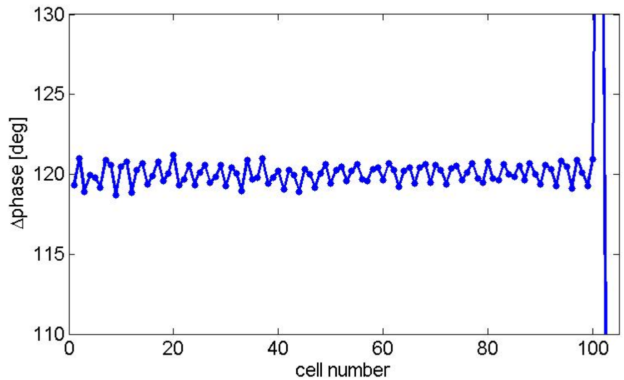

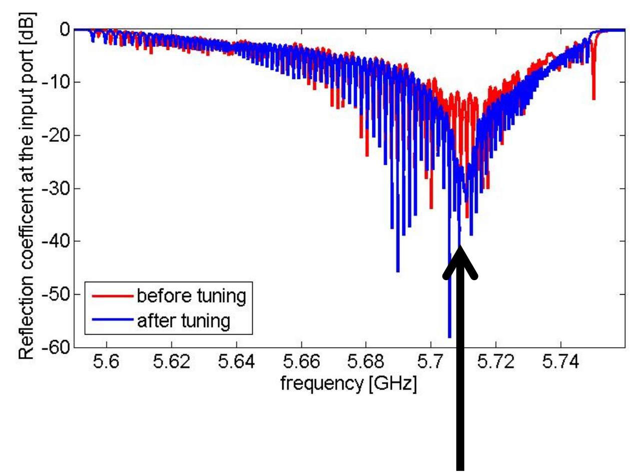

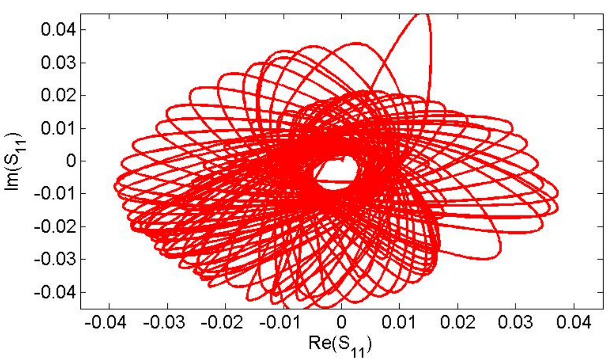

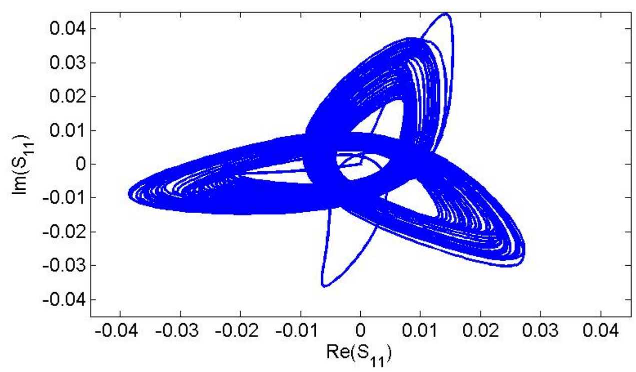

<-25 dB

C-BAND STRUCTURES: HIGH POWER TEST SETUP

The structure has been tested at **high power at the Bonn University under RI responsibility**.

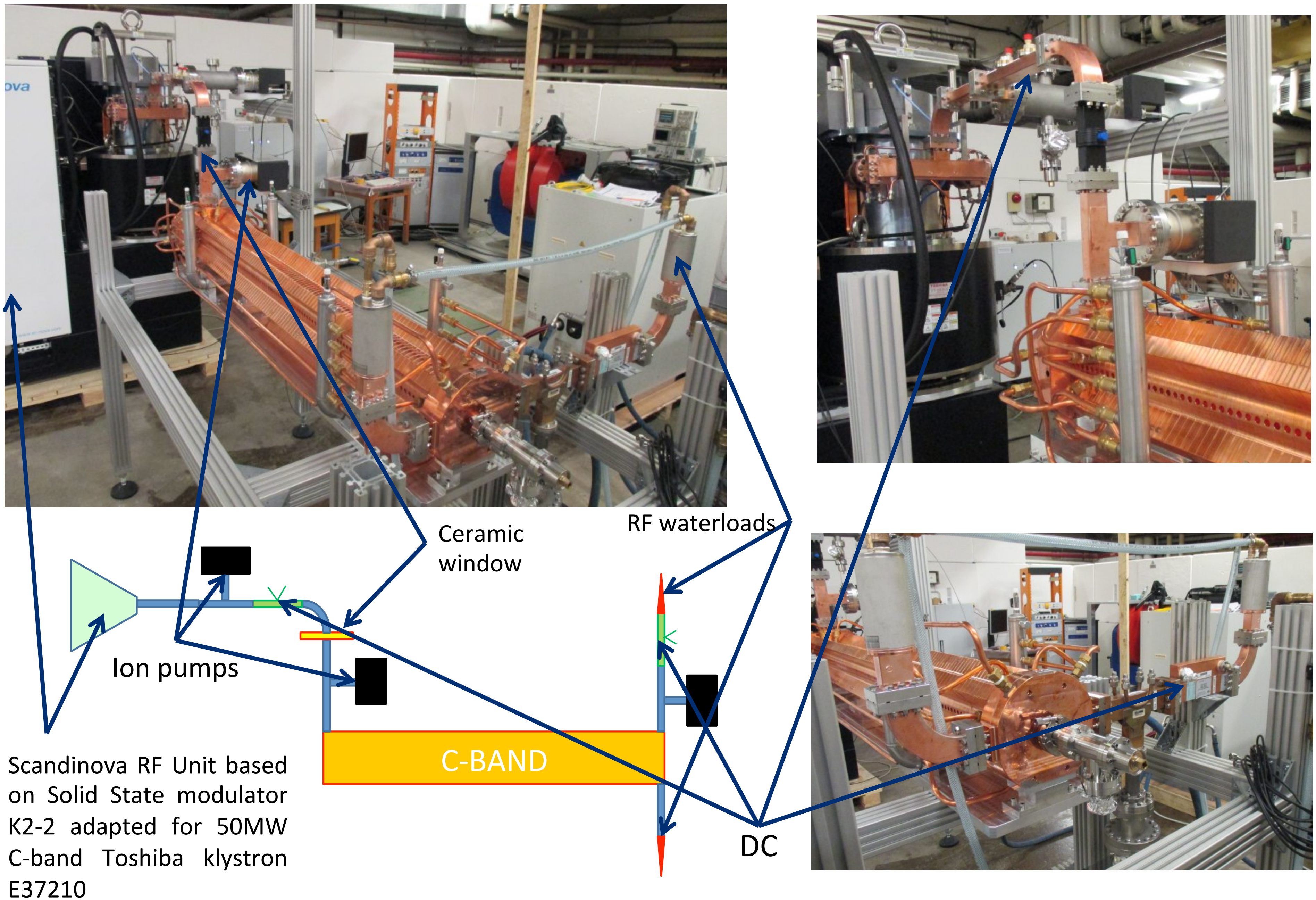

C-BAND STRUCTURES: HIGH POWER TEST RESULTS (1/2)

The aim of the RF conditioning is to reach **40 MW** at the input coupler at **100 Hz** repetition rate and **820 ns** pulse width. The **conditioning started at 10 Hz, 100 ns** input pulse and minimum power. The **forward/reflected power signals** at the input coupler and output coupler were measured using diodes from INFN and an oscilloscope. These readings were recorded to the Labview GUI which calculates the corresponding power levels.

The conditioning of the structure **started on 18.03.2015 and ended on 23.04.15**. The klystron power was progressively increased (by increasing the HV of the modulator) and the current of three ion pumps connected around the structure and the RF signals from pickups were monitored.

The **conditioning procedure was semi-automatic** and the switch-off on the HV were caused by:

(a) operators;
(b) threshold on the ion pumps current absorption (>$1x10^{-7}$ mBar)
(c) reflected power to the klystron exceeding a certain threshold.

The RF conditioning for the first RF structure lasted about **190 hours**

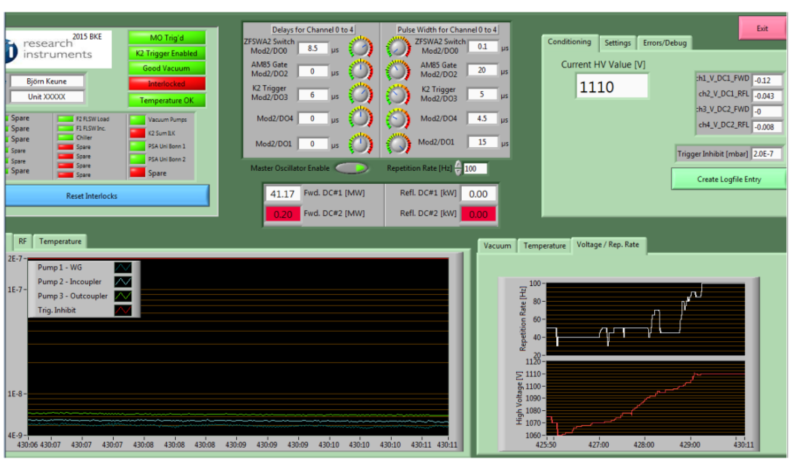

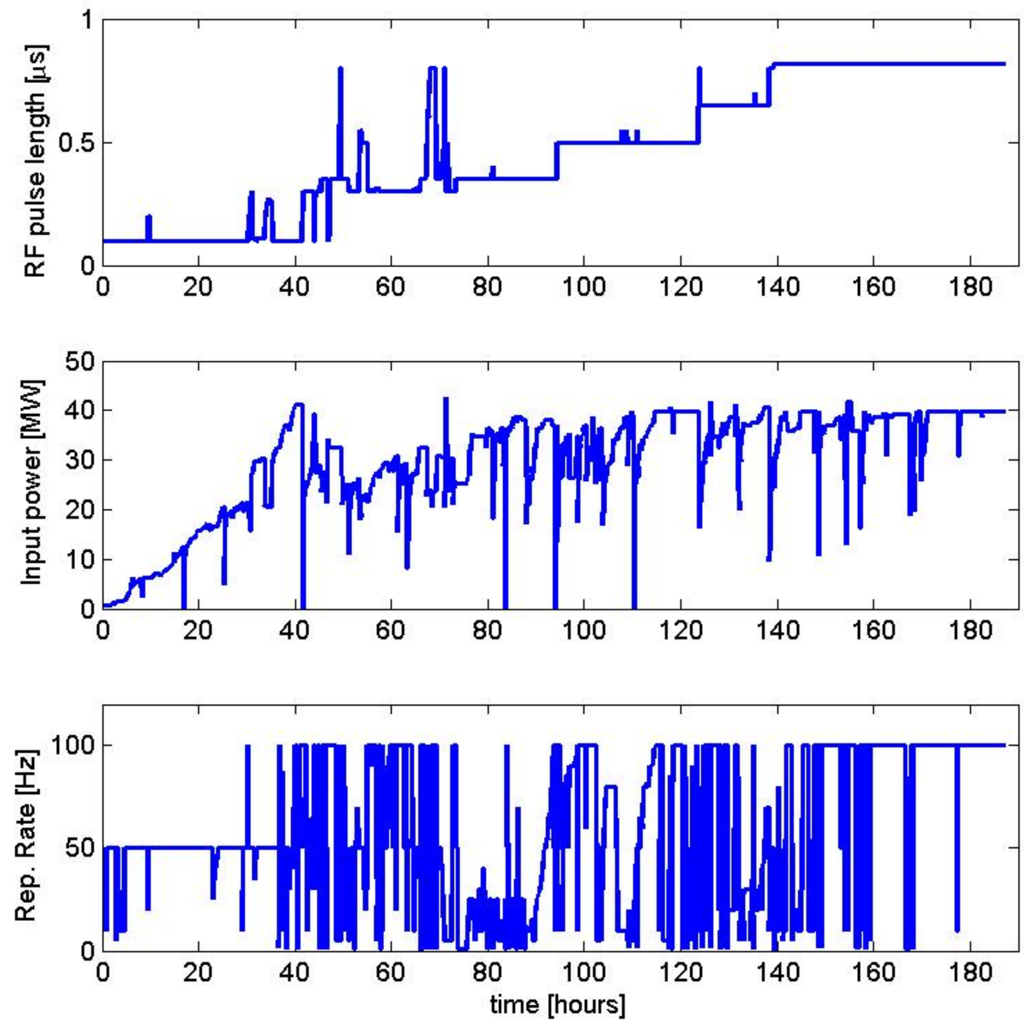

C-BAND STRUCTURES: HIGH POWER TEST RESULTS (2/2)

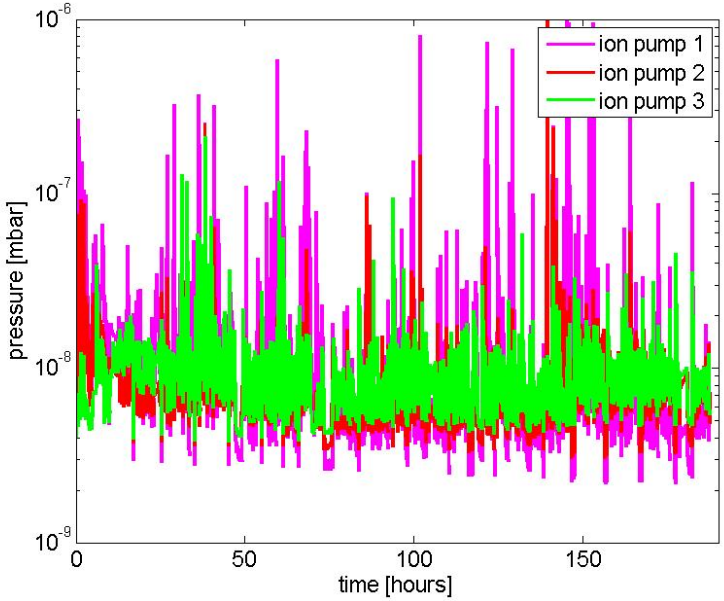

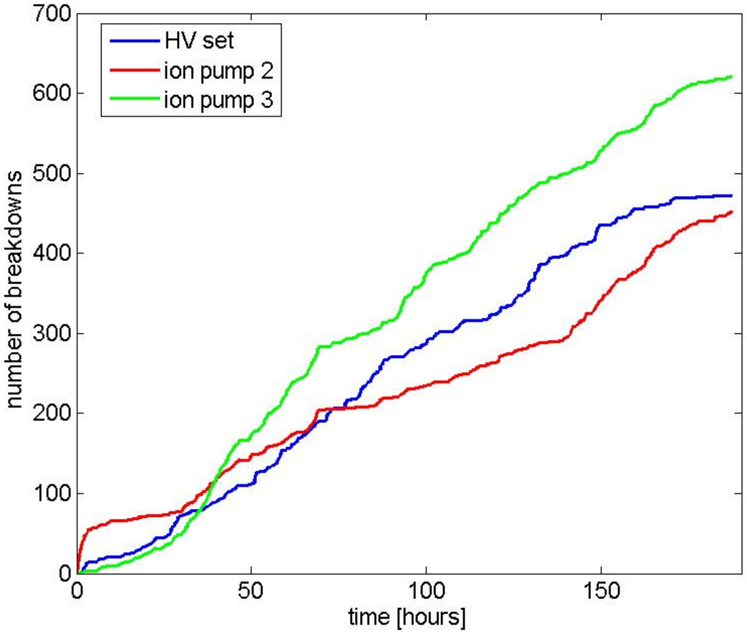

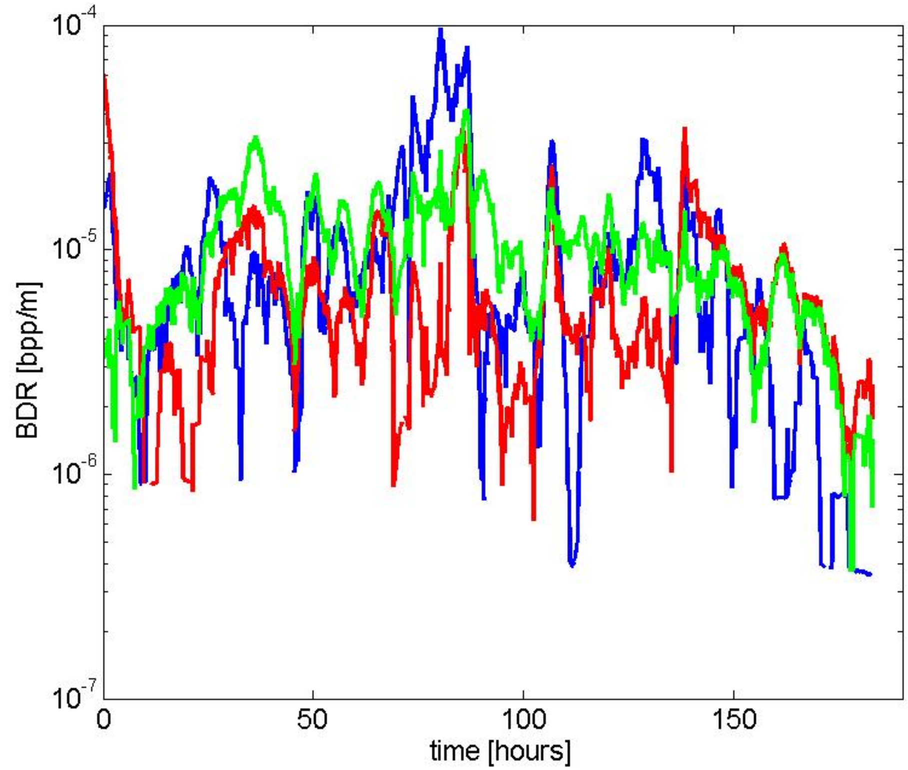

RF GUN

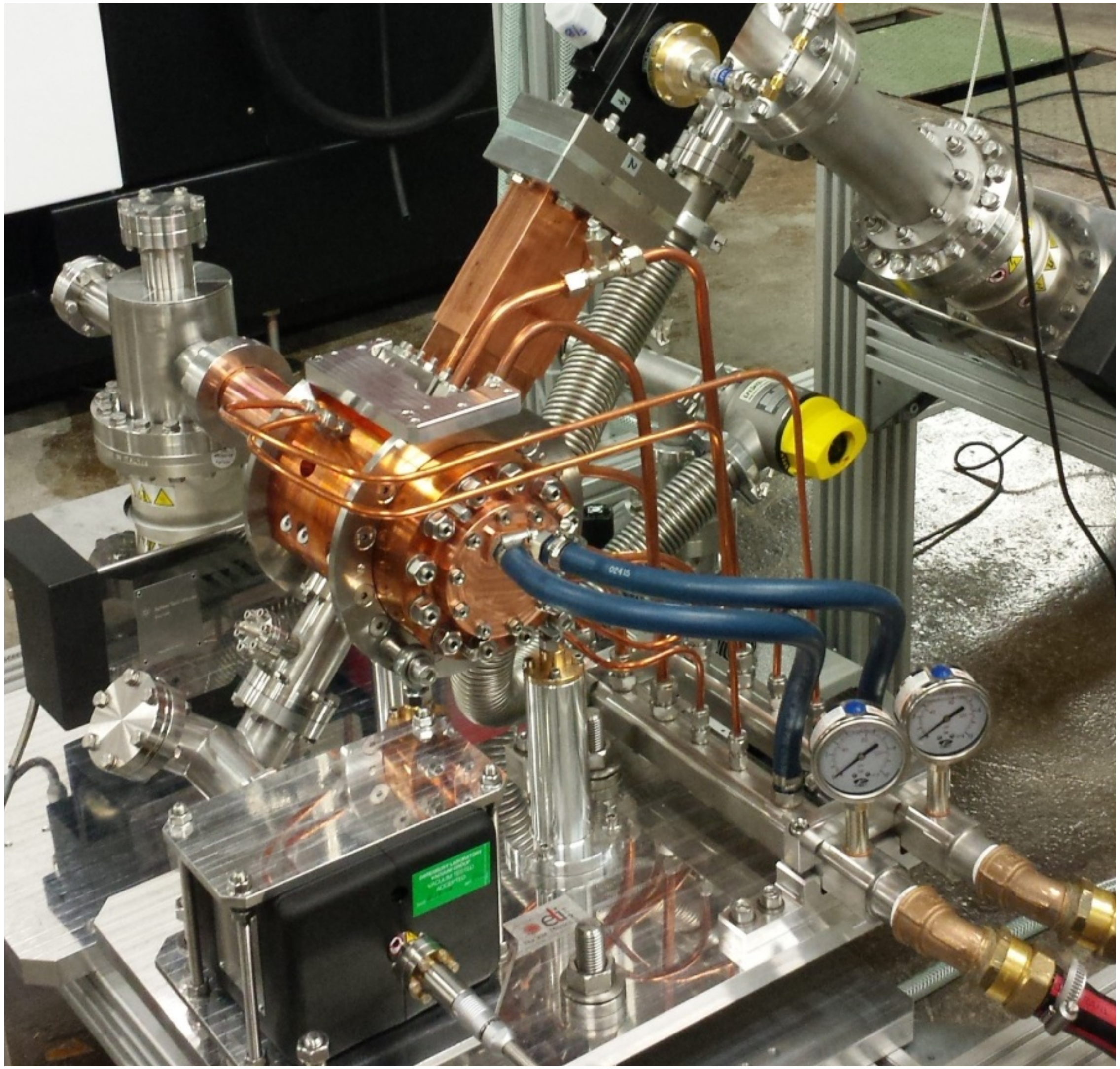

D. Alesini et al., PRST-AB 18, 092001 (2015)

INTRODUCTION

Photocathode RF guns are **multi-cell SW structures**. The **electron beam is generated by photo-emission** using a drive-laser pulse to illuminate the cathode. These devices find several applications (FELs, THz sources, Compton sources…). The **peak field** at the cathode is directly proportional to the maximum achievable beam **brightness**.

In the last generation of RF guns much effort has been spent to **increase the peak E field amplitude (proportional to the achievable emittance) reducing the BDR**

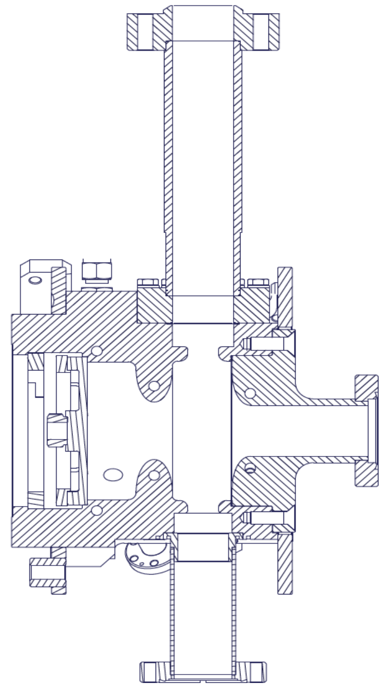

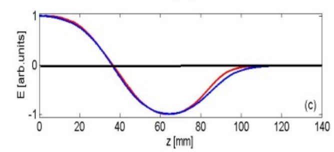

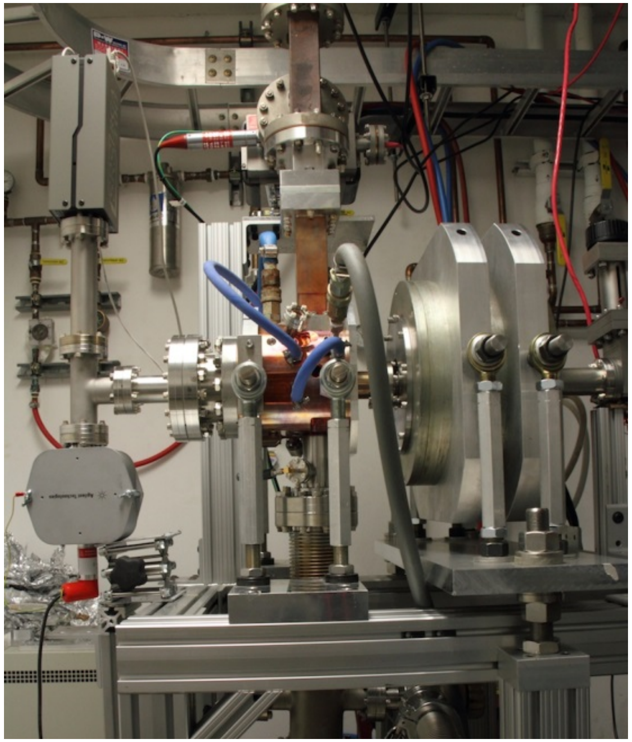

Realization process

The RF guns are realized by a **brazing process** following all **cleaning procedure of the high gradient technology**. But brazing process:

⇒ requires large vacuum furnace
⇒ is very expensive
⇒ poses a not negligible risk of failure.
⇒ at the end of the process the copper is "soft"

RF design

⇒ **couplers** with reduced pulsed heating
⇒ **irises** profiles with lower peak surface electric field.
⇒ **increase of the modal separation** between the π and the 0 mode to fed the gun using very **short RF pulses**.

NEW DESIGN AND REALIZATION OF THE SPARC GUN

The new RF gun has been built as a replacement of the SPARC-LAB injector.

⇒For the novel gun design the **iris profile** has been designed with an **elliptical shape** and a **large aperture** to simultaneously reduce the peak **surface electric** field, increase the **frequency separation** between the two RF gun modes and increase the pumping speed on the half-cell.

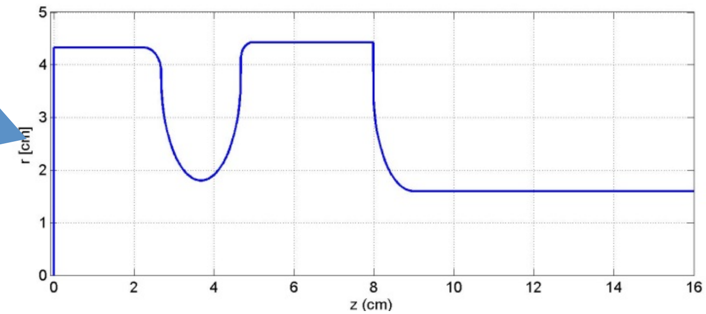

⇒The **coupling window** between the rectangular waveguide and the full cell has been strongly rounded to **reduce** the peak surface magnetic field and, as a consequence, the **pulsed heating**.

⇒Furthermore, the new SPARC GUN has been **realized without brazing** using a novel process recently developed at LNF-INFN involving the use of **special gaskets** that guarantee (simultaneously) the vacuum seal and perfect RF contact when the structure is clamped.

r_{iris}	18 (mm)
t	20
b_{half}	43.23
b_{full}	43.675
r_{pipe}	16
L_{half}	36.74
L_{full}	53.04

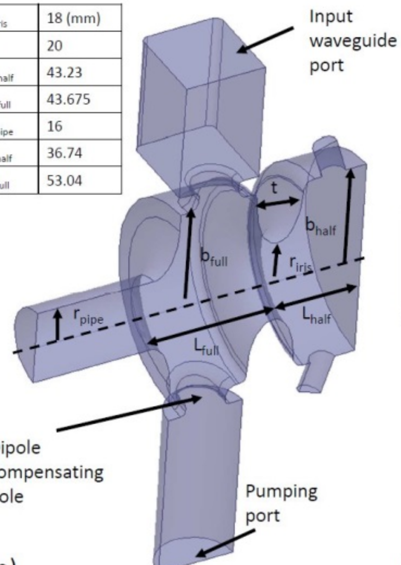

(a)

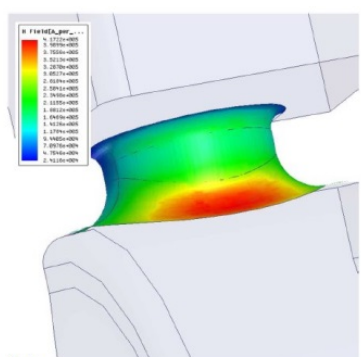

(b)

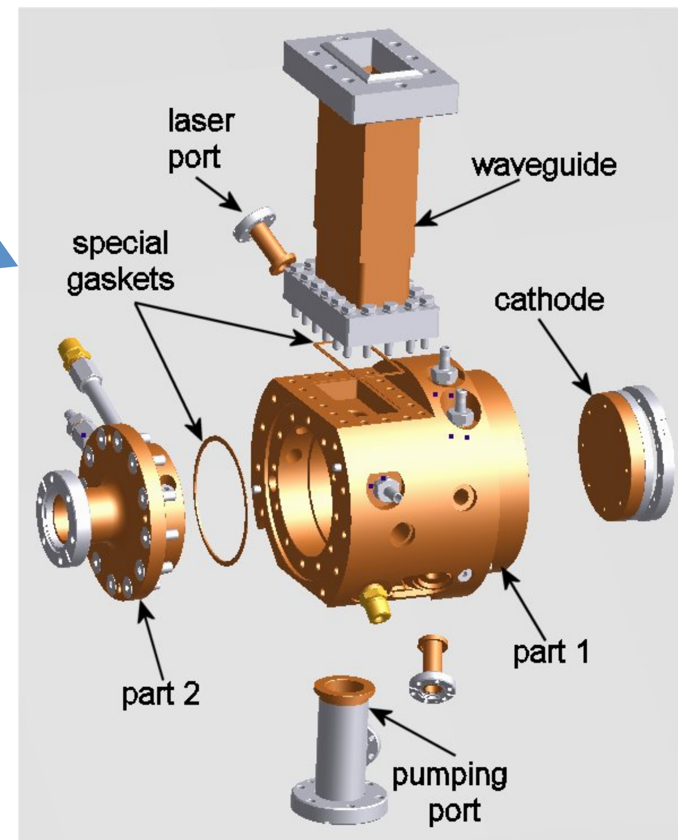

FINAL GUN PARAMETERS

Parameters	Theoretical (HFSS)	Measured
f_{res}	2.856 [GHz]	
Q_0	15300	15000
Coupling β	2	1.7
Shunt impedance (R)	1.78 [MΩ]	
$E_{surf\_peak}/E_{cathode}$	0.85	
$E_{cathode}/\sqrt{(P_{diss})}$	38 [MV/m/MW$^{0.5}$]	
Frequency separation between the 0 and the π-mode	39 [MHz]	39.6 [MHz]
H_{surf_peak} @ $E_{cathode}$ =120 MV/m	420 [kA/m]	
Pulsed heating (2 μs RF pulse length)	<55 [°C]	
Field flatness	<1%	<5%
Repetition rate	10 [Hz]	
Average dissipated power	75 [W]	
Working temperature	20 [°C]	

FABRICATION PROCESS (1/2)

The gun has been fabricated with a **new technique recently developed at LNF that does not involve any brazing step**.

The **body of the gun** (part 1) has been fabricated from a single piece of OFHC copper using diamond tools.

The **rounded coupler geometry has been realized with a 5 axis milling machine**.

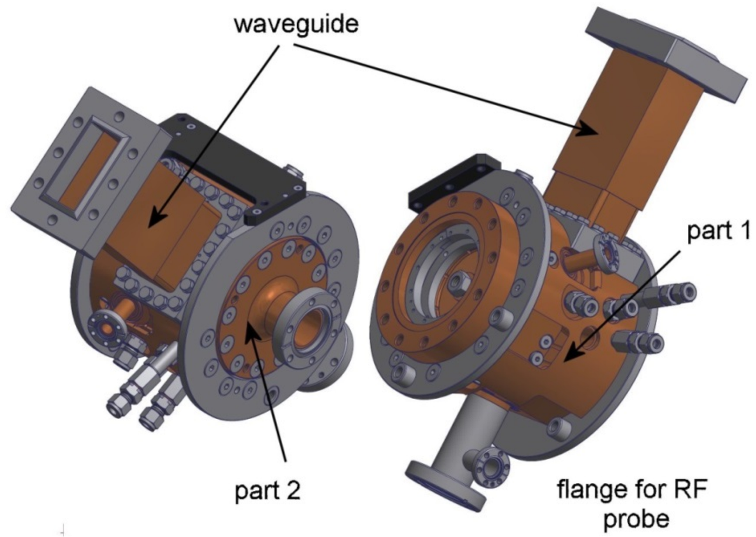

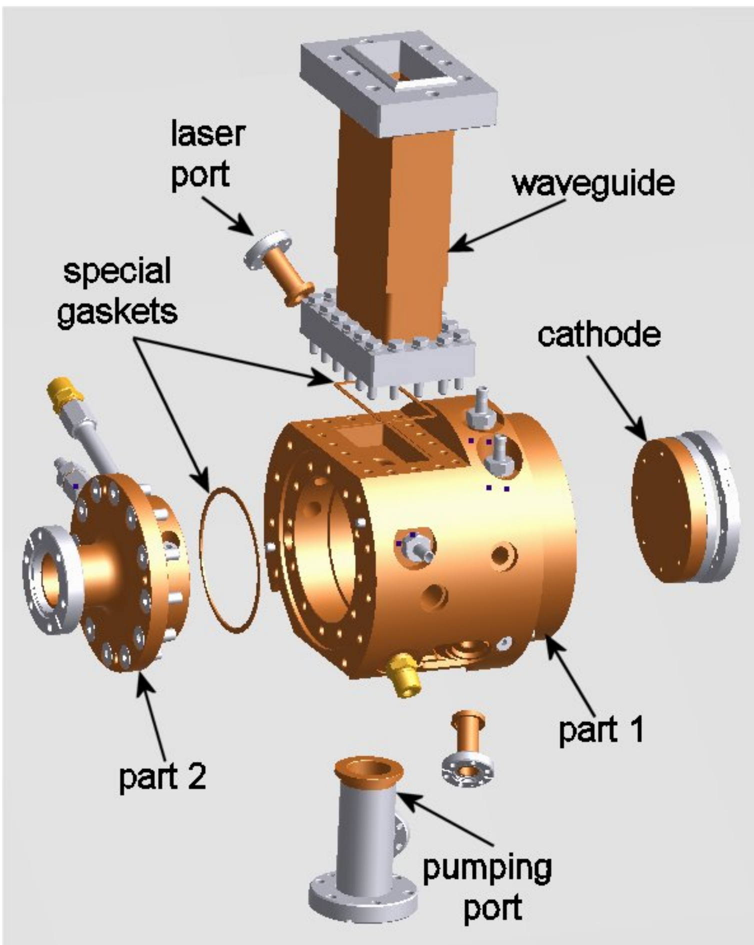

The full cell has then been sealed clamping the body of the gun with the closing cap (part 2) and using the **special gasket** developed at LNF-INFN that simultaneously guarantees **the vacuum seal and the RF contact** avoiding sharp edges and gaps.

The waveguide has been fabricated separately and the RF contact and vacuum seal between the waveguide and the body of the gun has been obtained using another gasket**.**

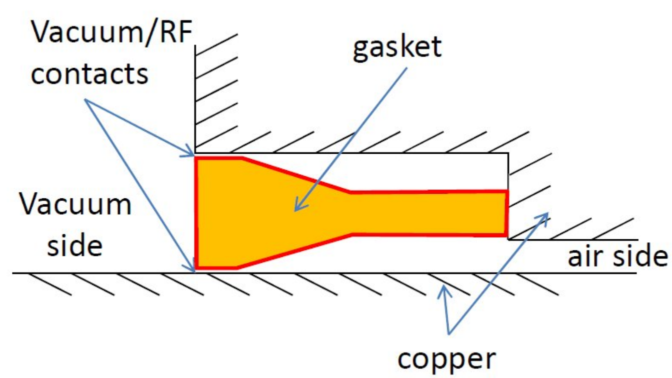

Int'l patent application PCT/IB2016/051464

FABRICATION PROCESS (2/2)

The device has been fabricated with a **precision on the internal dimensions of +/- 10 μm** while the surface roughness is maintained smaller than 200 nm.

Before the final clamping, the gun has been **cleaned** with a detergent (ALMECO-19) and a mixture of organic (citric) acid and distilled water, in a bath with an ultra-sound machine.

After the assembly a **bake-out at 150 deg for 24 hours** allowed reaching a vacuum pressure below **$5 \cdot 10^{-10}$ mbar**.

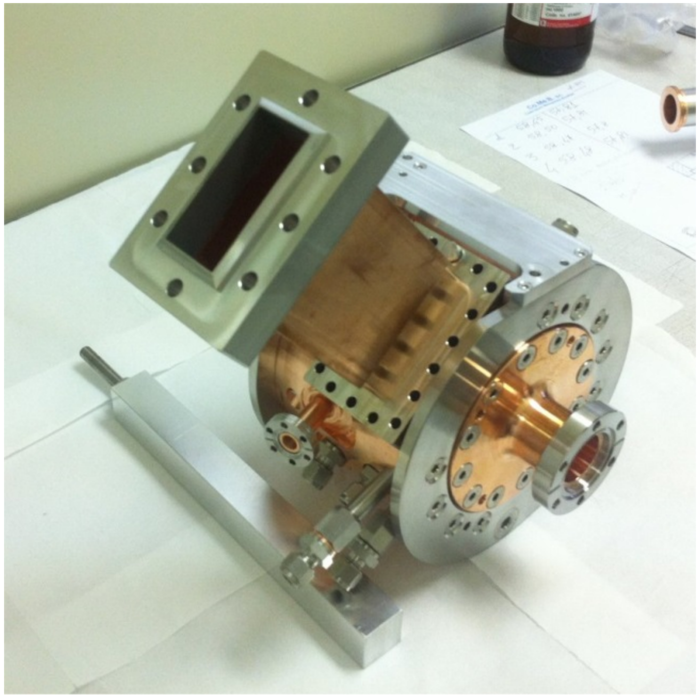

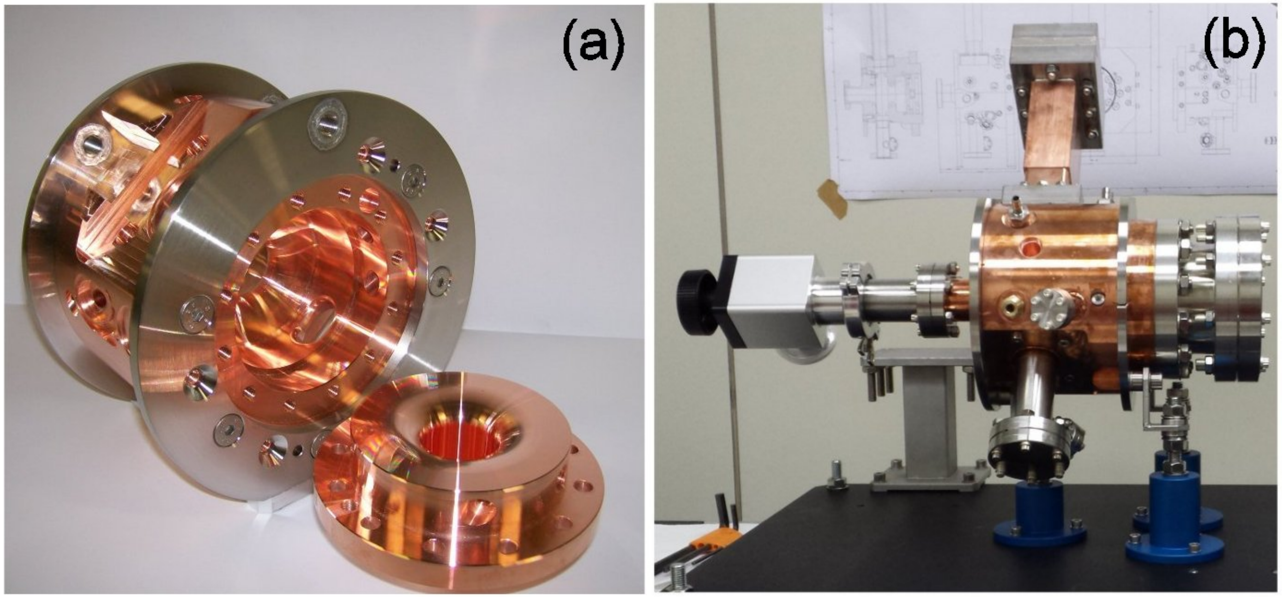

LOW POWER RF MEASUREMENTS

Low power RF test and tuning of the gun have been performed using a Network Analyser and the bead drop technique.

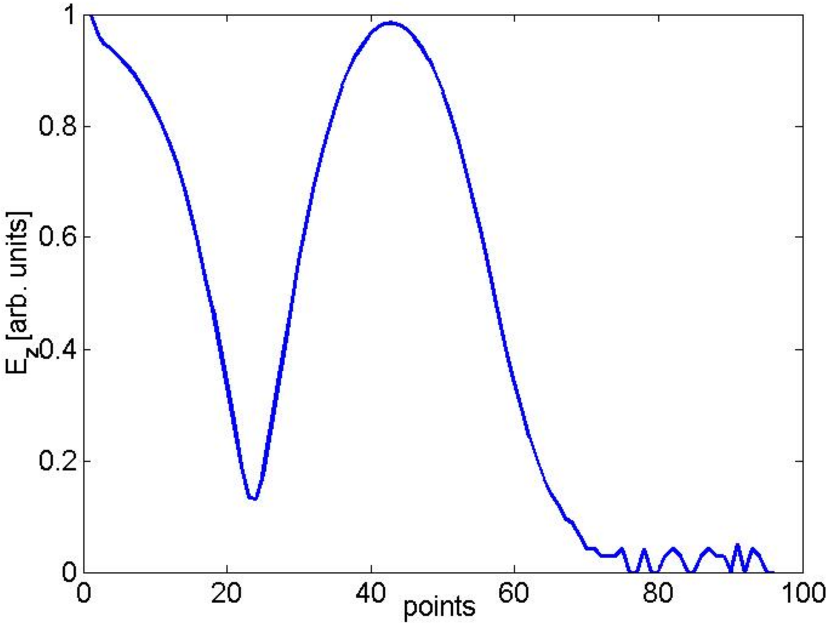

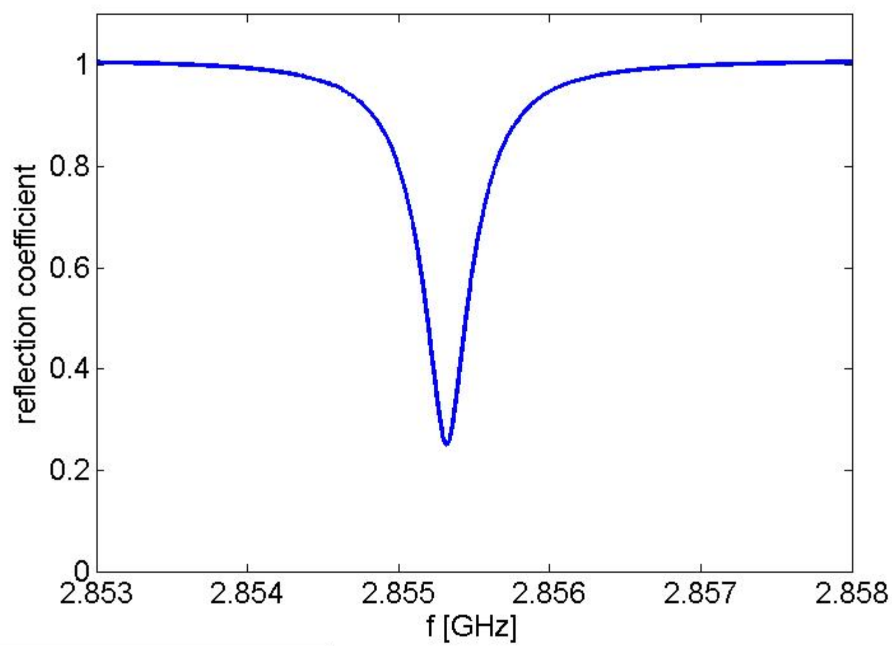

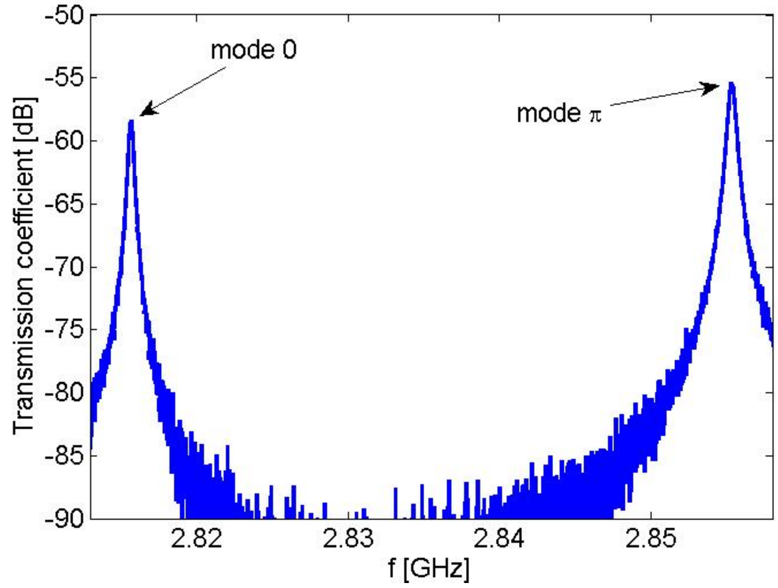

INSTALLATION AT UCLA FOR HIGH POWER TEST

High power RF tests have been performed at the University of California Los Angeles (UCLA) in the framework of a collaboration between INFN-LNF and UCLA.

The gun has been installed in the **Pegasus Laboratory** and has been conditioned for about 5 weeks.

The structure has been fed by an **XK5 klystron that was able to give a maximum power of 10 MW with a maximum rep. rate of 5 Hz** and a variable RF pulse length up to 2 us.

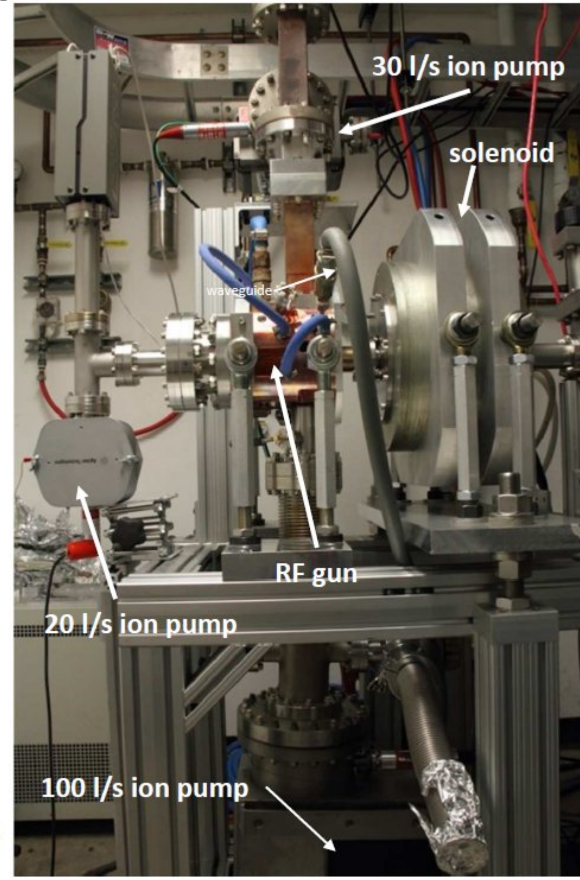

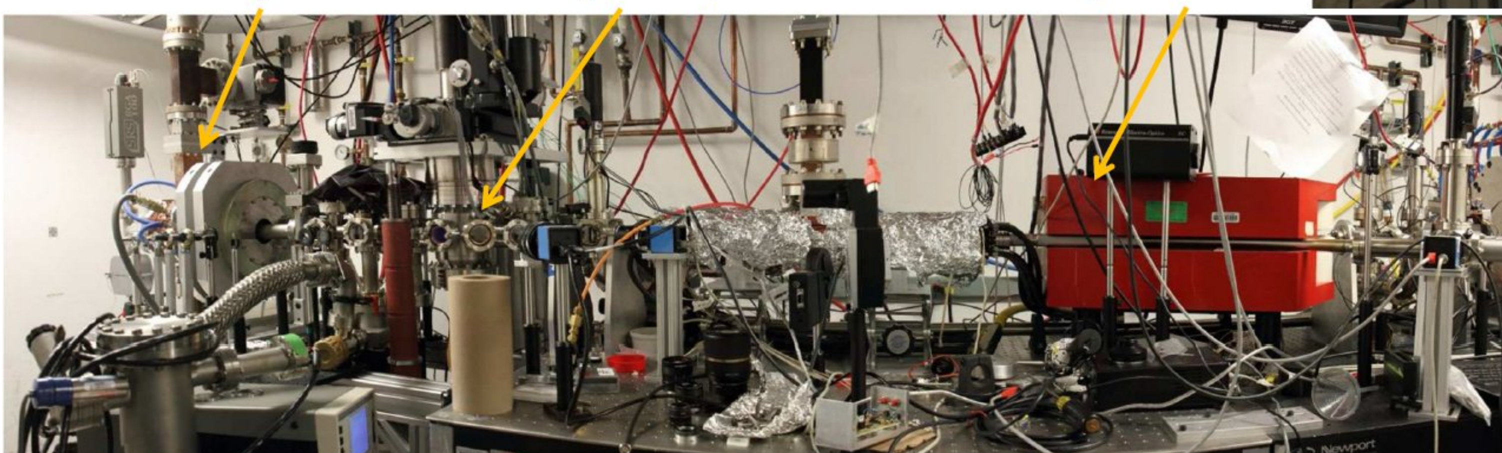

HIGH POWER TEST RESULTS

The conditioning has been done for about 8 hours per day (working days) with a **total amount of about 80 hours**.

The power and the RF pulse length have been progressively increased starting with a short pulse length of 1 μs.

The gun reached **about 8 MW of maximum input power with an rms pulse length of 2 us** , corresponding to a **92 MV/m** cathode peak field. The conditioning to higher fields was mainly limited by the available RF power.

Moreover even if the RF gun has been designed to operate with very short RF pulses and high peak power, the klystron reach power up to 10 MW only for long pulse length (>2.5 μs). This element is not ideal when trying to push for high gradients.
A full conditioning at the low repetition rate of 5 Hz requires a very long time to reach the final BDR.

In the very short conditioning period we reached at the end a **BDR <5x10^{-6}**

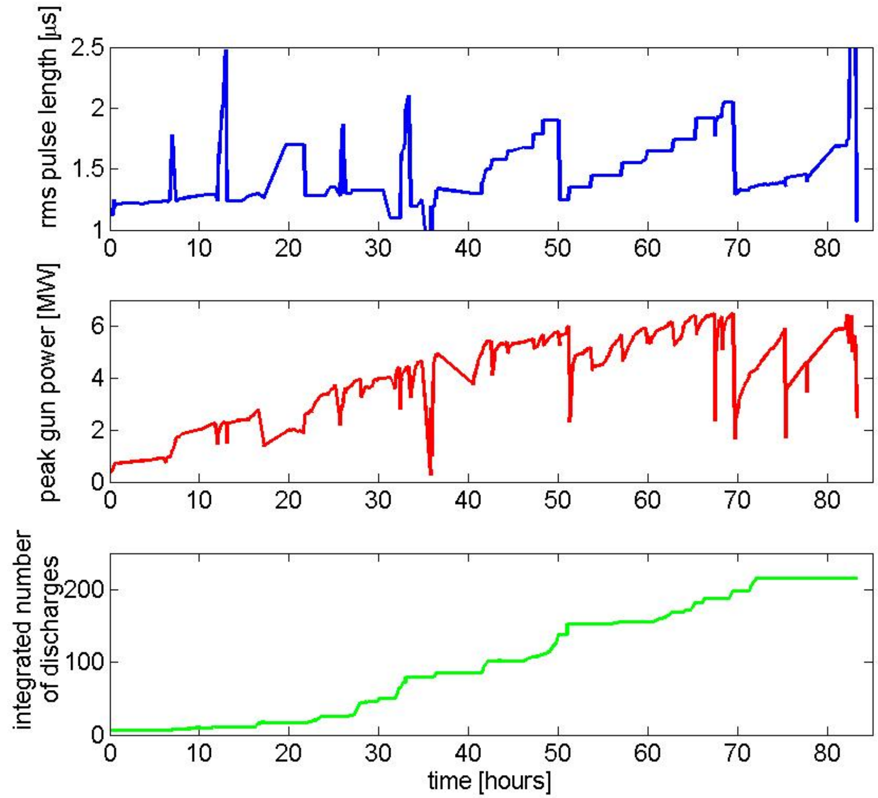

The **GUN is now used for experiments** mainly on electron diffraction at UCLA

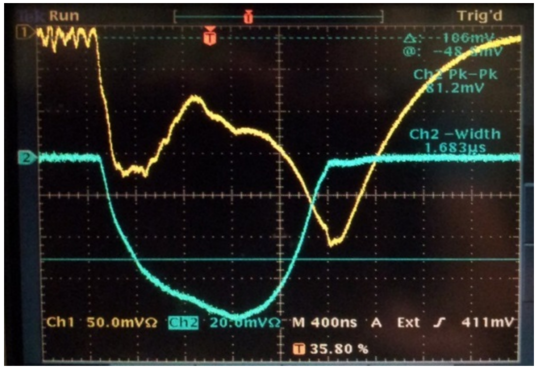

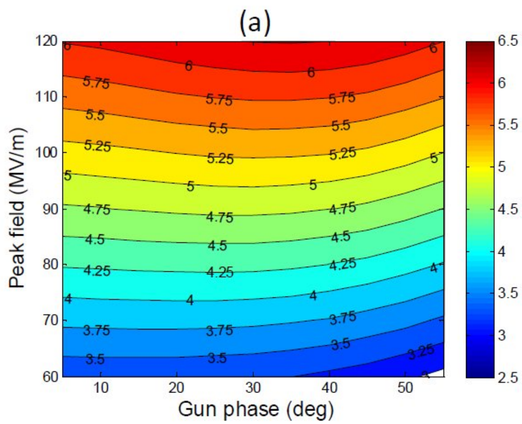

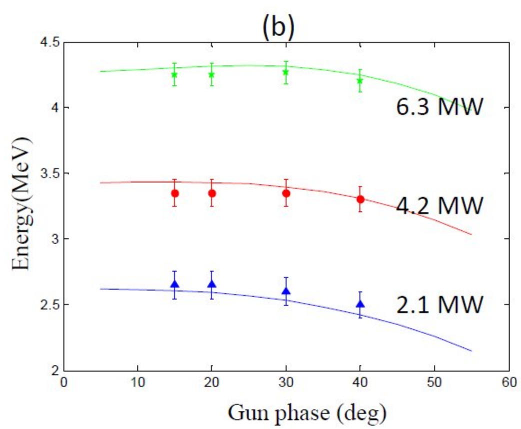

ELI-NP GUN

The **RF GUN of the ELI NP GBS** has been fabricated similarly to the new SPARC gun but with a couple of different features:

1) ***Large amount of cooling channels (100 Hz operation)***
2) ***Cooled cathode***
3) ***Coupling coefficient β=3 (short RF pulses)***
4) ***NO laser port at 72 degree (like SPARC)***
5) ***The pipe flange is a special flange to avoid EBW/soldering/brazing***
6) ***Waveguide and pumping port junctions have special gaskets to avoid welding/brazing***

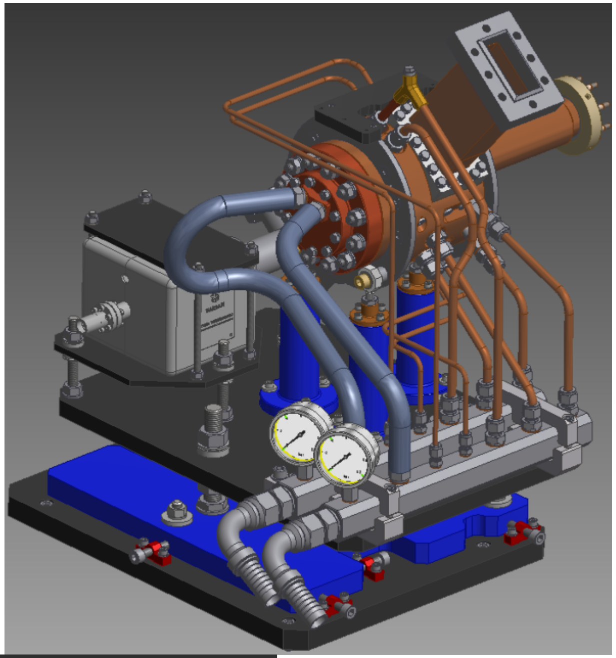

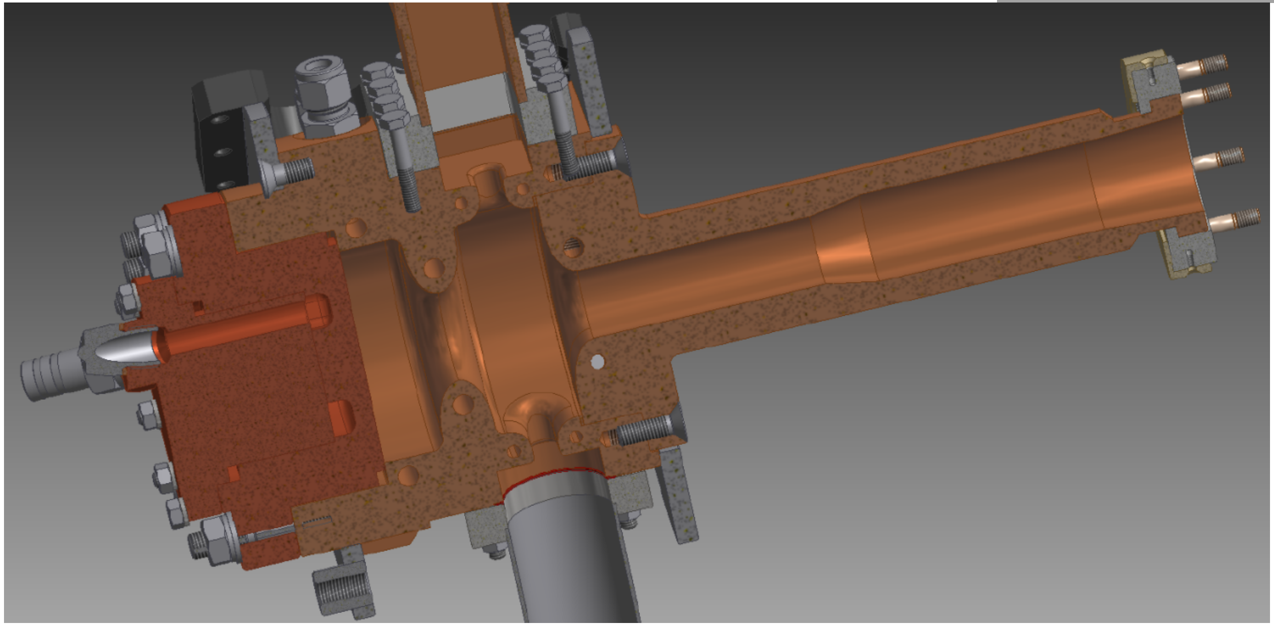

S BAND GUN: PARAMETERS

RF frequency	GHz	2.856
Repetition frequency	Hz	100
Working mode		π SW
Max RF input power	MW	16 (shaped)
RF peak field at the cathode	MV/m	120
Max RF pulse duration	μsec	2 (1.5 nominal)
RF pulse duration for beam	μsec	0.5
Unloaded Q factor		14600
Average dissipated power	kW	1.3
Working temperature	degrees	34
Coupling coefficient		3
Filling time	μs	420
Shunt impedance	MΩ	1.64
Operating vacuum pressure	mbar	$1\text{-}5\cdot10^{-9}$
Number of cells	#	1.6
Type of cathode		copper
Cathode quantum efficiency @ 266 nm		$>2\cdot10^{-5}$

RF GUN THERMAL DESIGN AND CATHODE

A detailed thermal analysis has been performed to investigate the impact of the 100 Hz operation. The average dissipated power in the gun is 1.5 kW. Also the cathode is cooled.

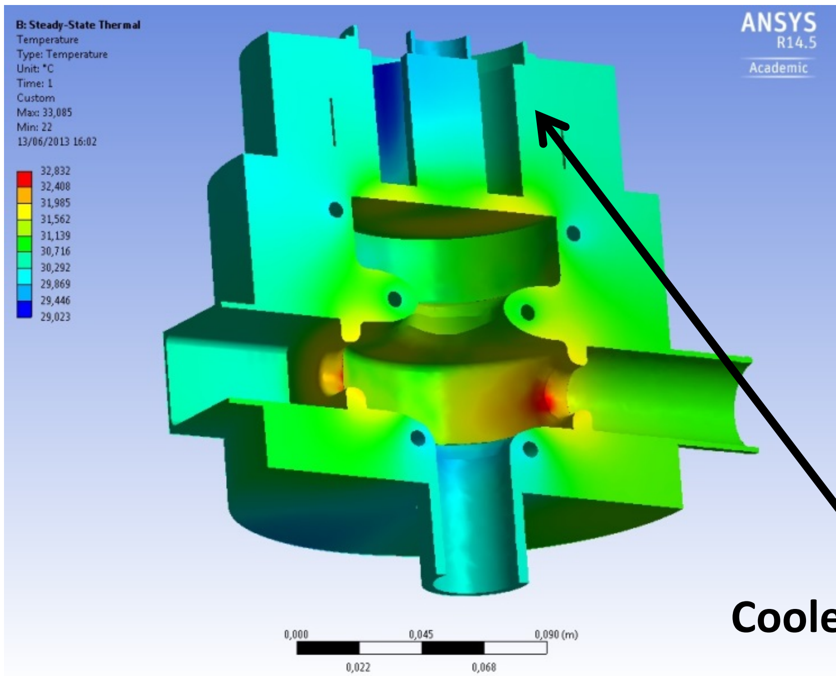

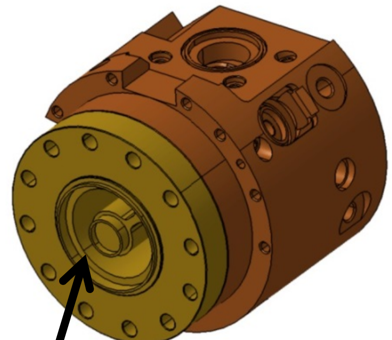

Cooled cathode

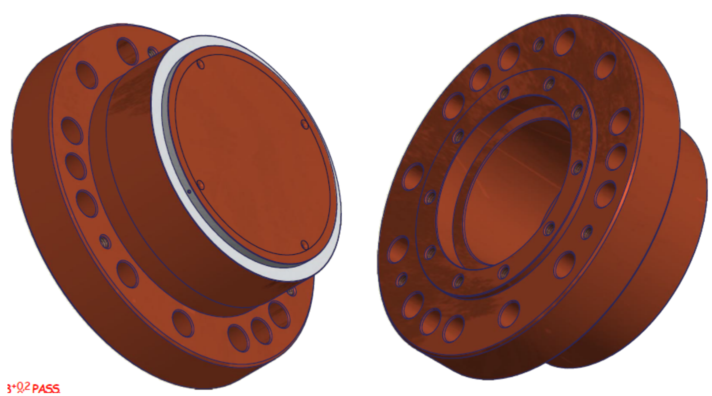

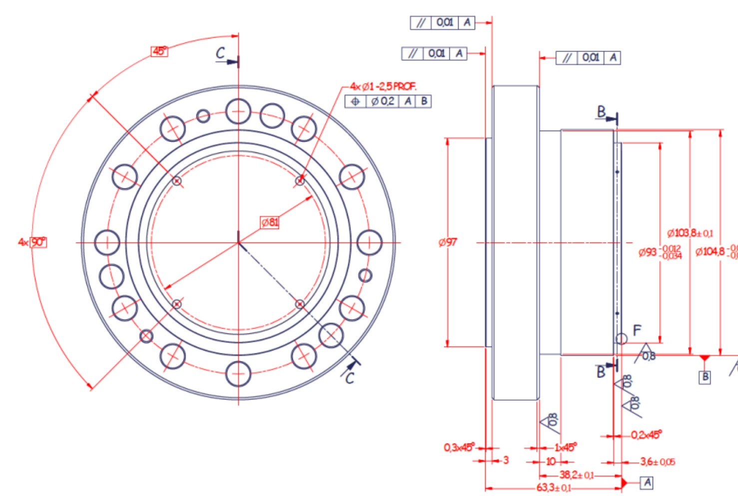

S-BAND GUN: ASSEMBLY

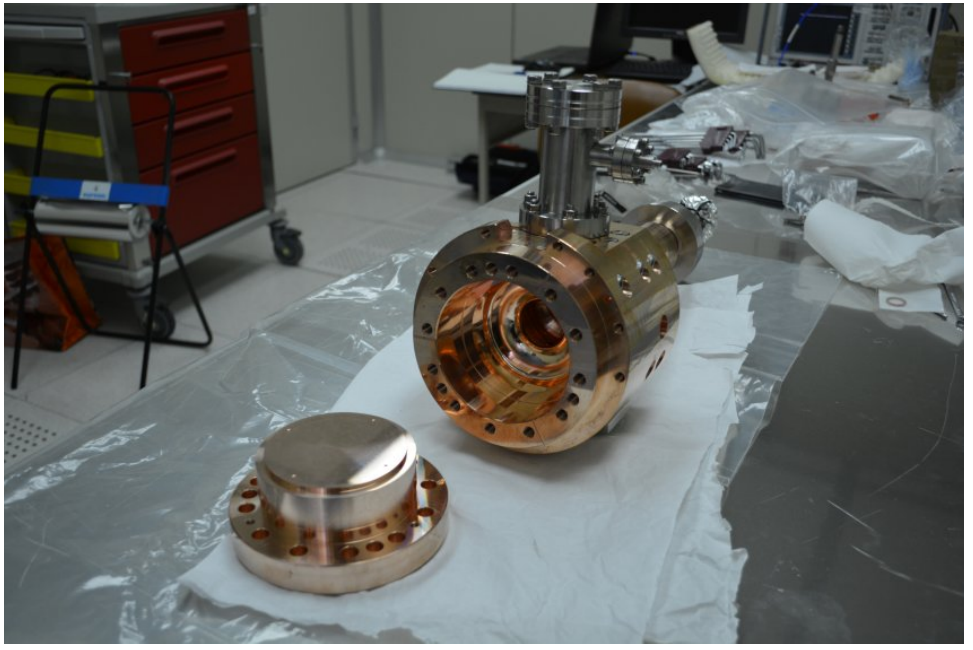

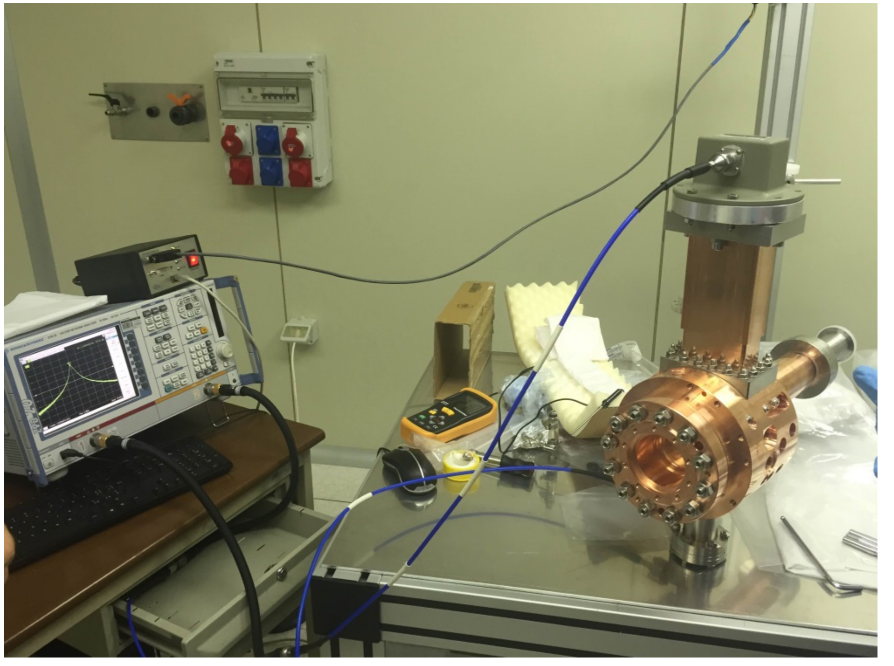

S-BAND GUN: LOW POWER RF TEST

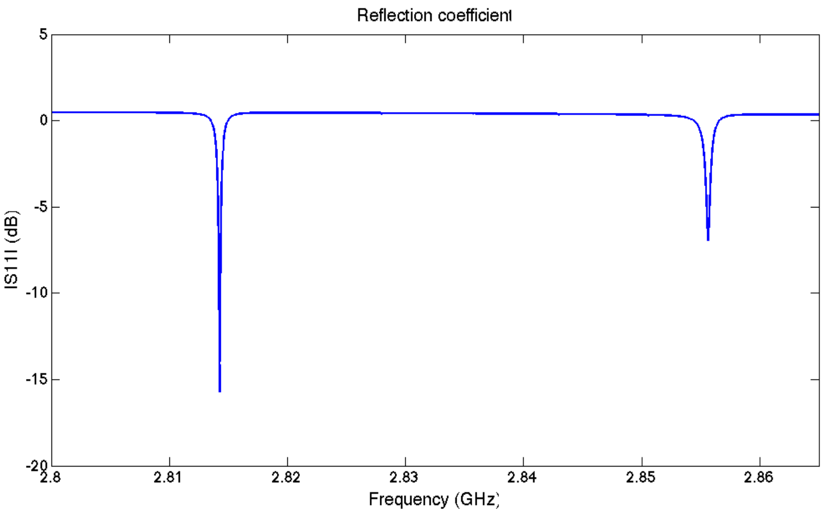

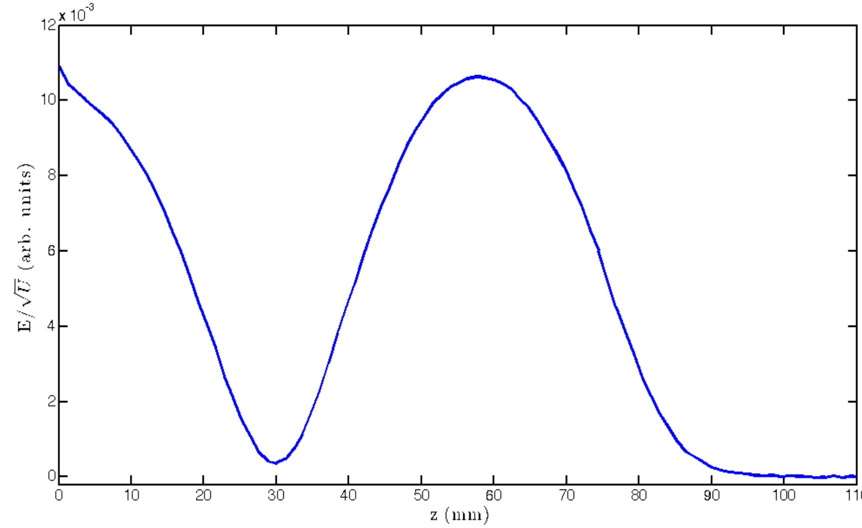

Parameter	Value
resonant frequency (f_{res})	2.856 GHz @34 deg
reflection coeff. @ f_{res}	-6.9 dB
coupling coeff. (β)	2.64 (3)
unloaded Q	14980
loaded Q	4115
0/π mode separation (Δf)	41.3 MHz

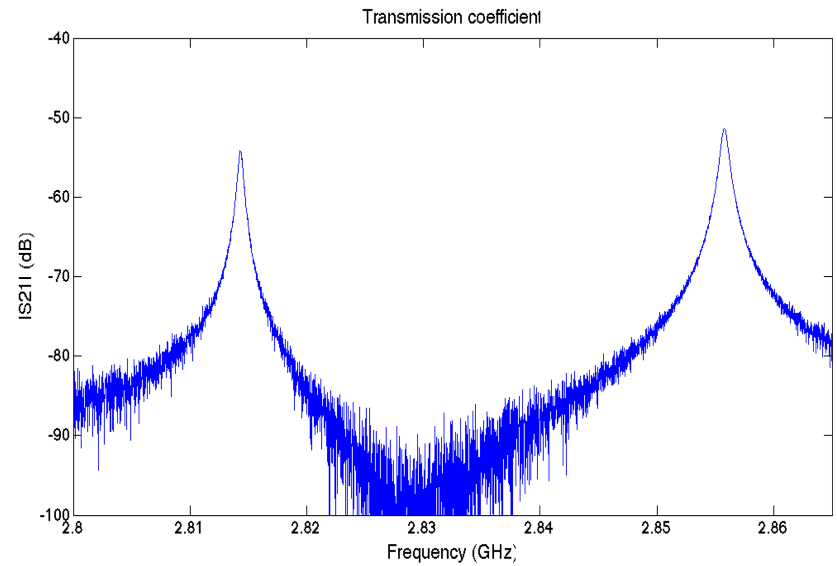

S-BAND GUN: HIGH POWER RF TEST (@ BONN)

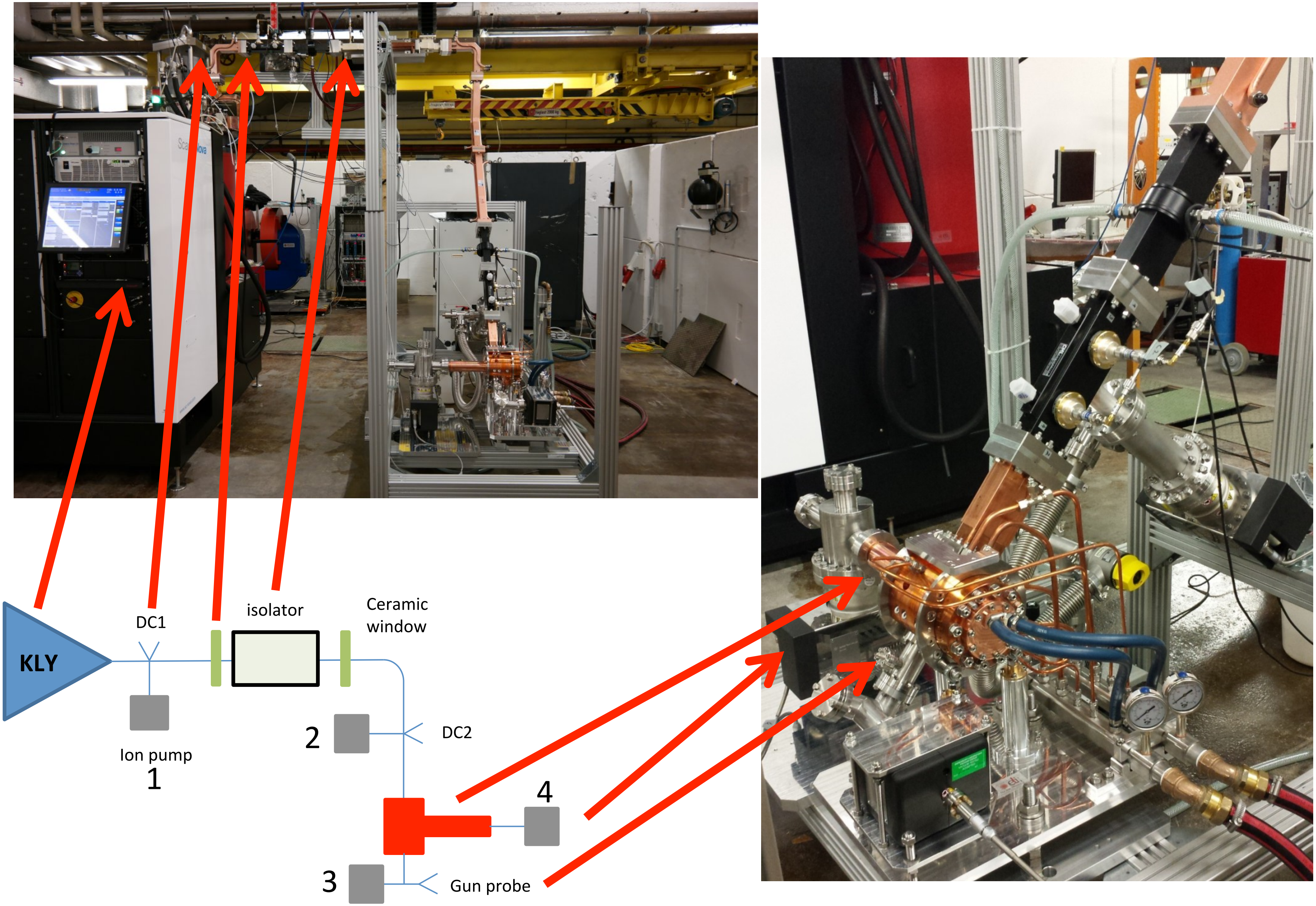

S-BAND GUN: HIGH POWER TESTS RESULTS

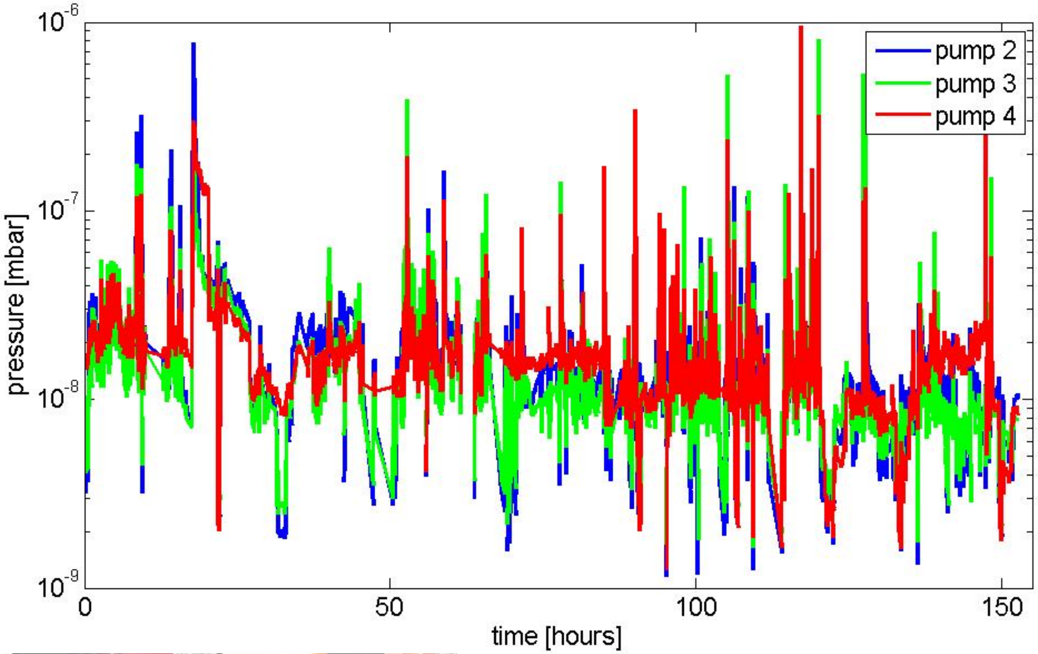

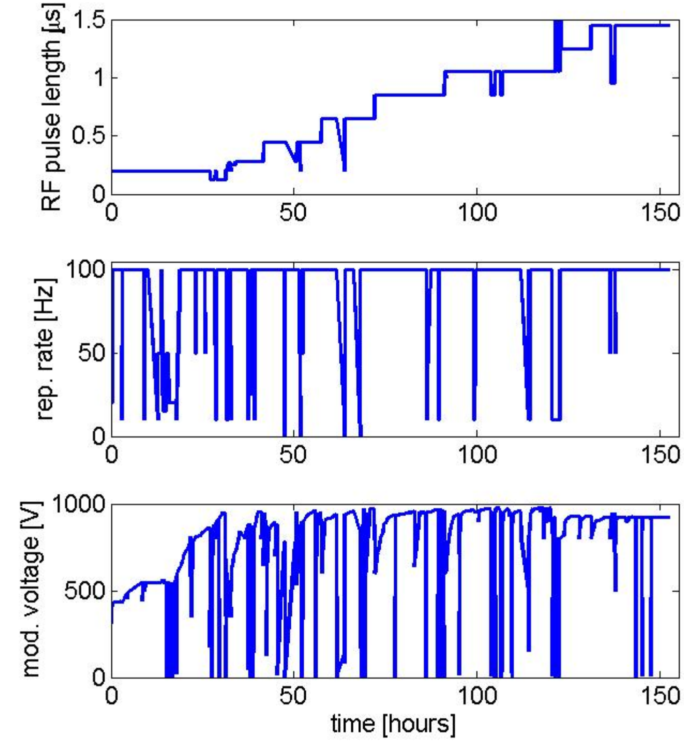

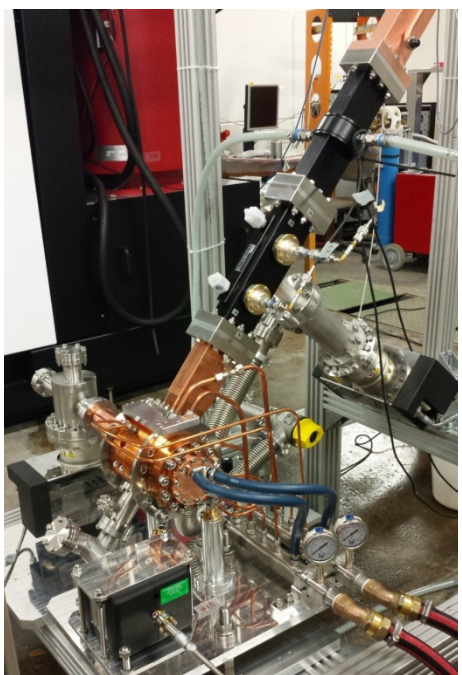

Full parameters have been achieved in a very short time with overall extremely good performances

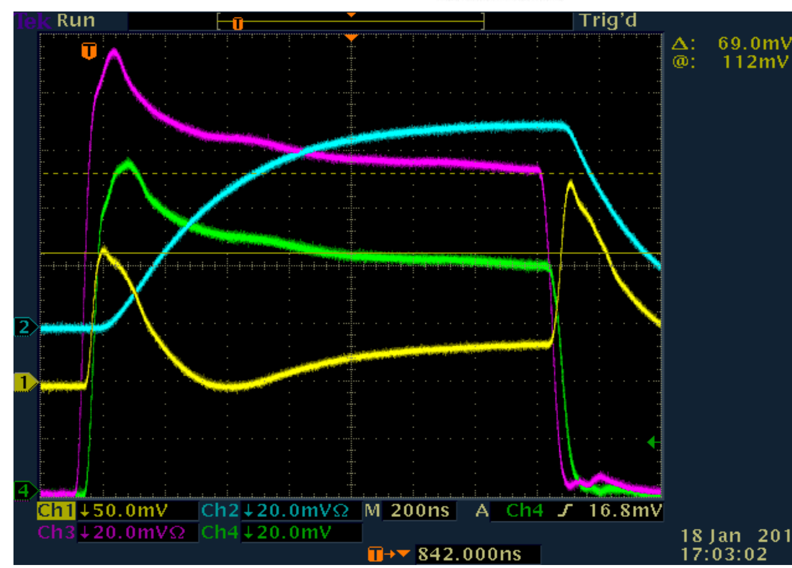

WHAT NEXT: LINAC WITH GASKETS

The gaskets technique has been successfully applied for the realization of both the new SPARC_LAB 1.6 cells RF gun and the ELI-NP-GBS one. The results obtained for these devices in term of reached cathode peak field and BDR open the **possibility to successfully apply this technique to other rf structures**. To this purpose an S-band LINAC prototype with a reduced number of cells has been designed and will be fabricated and tested to demonstrate the feasibility of such approach also for LINACs. The prototype is a 10 cell S-band TW disk loaded accelerating structure, constant impedance with 2π/3 field phase advance per cell.

Dual feed input coupler with splitter

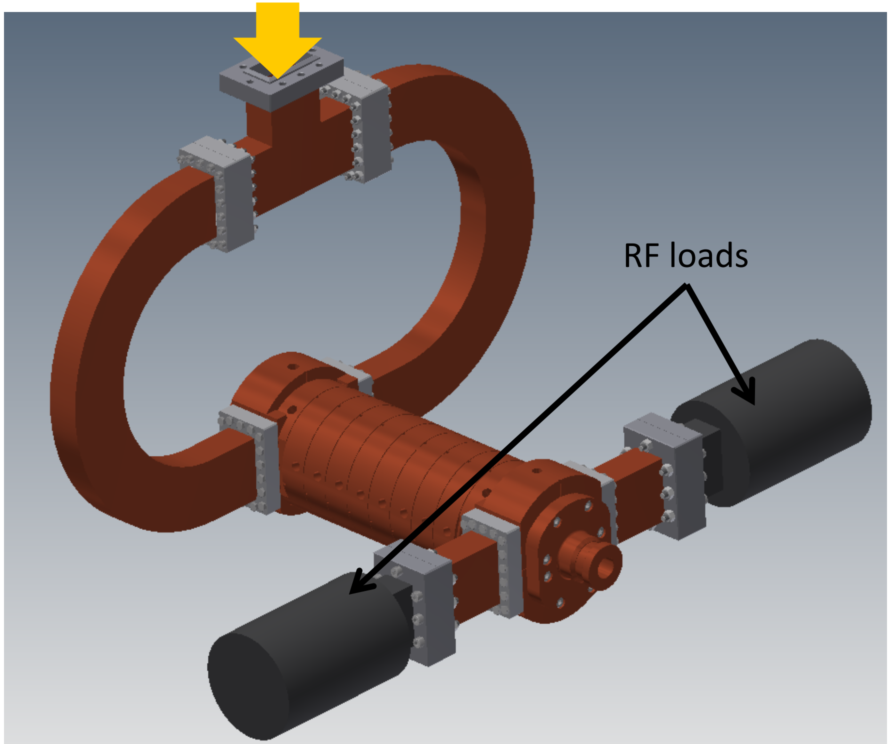

Frequency	2856 MHz
Phase advance per cell	2π/3
Number of cells	10
Cell Period	34.99 mm
Iris Radius	13 mm
Unloaded quality factor Q	14000
Group velocity (vg/c)	0.02
Field attenuation	$0.11\ m^{-1}$
Shunt impedance	11.61 MΩ/m
Series impedance	55 MΩ/m
$E_{acc}/\sqrt{P_{in}}$	$3.4\ MV/m/\sqrt{MW}$
s pulse leng	

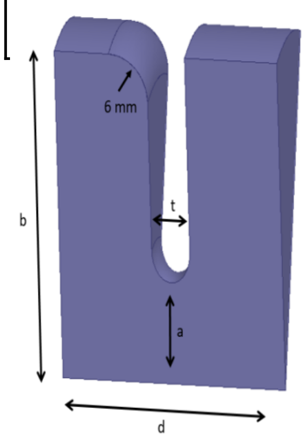

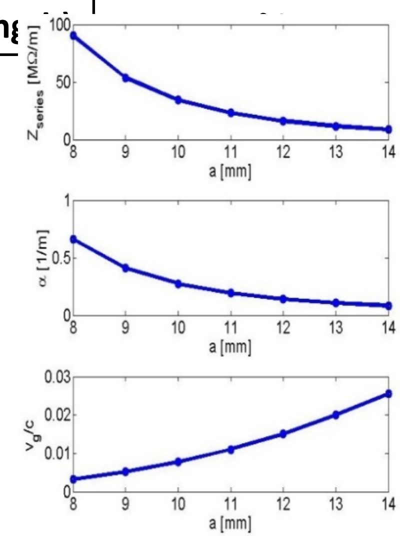

F. Cardelli *et al.,* proceedings IPAC16, MOPMW005.

LINAC WITH GASKETS: ELECTROMAGNETIC DESIGN

In the overall design a continuous **feedback between the electromagnetic design and the mechanical model** has been necessary.

Input/Output coupler design

- Dual feed (no dipole field)
- Racetrack profile with a «cut» to facilitate the machining and to compensate the quadrupole field components

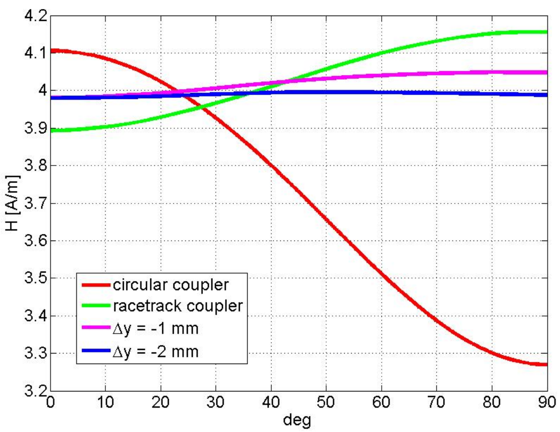

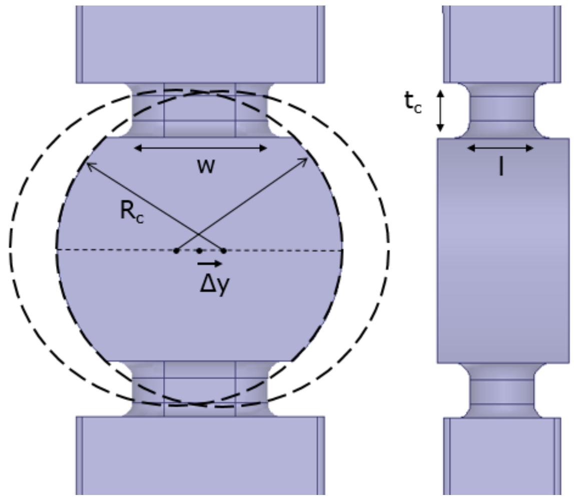

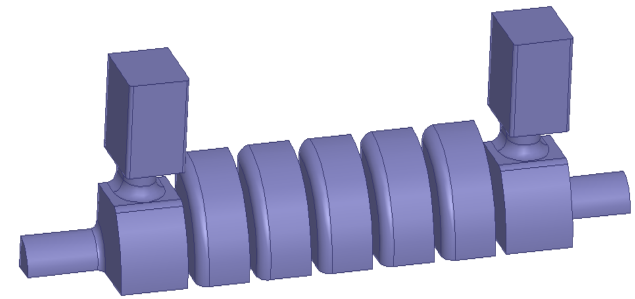

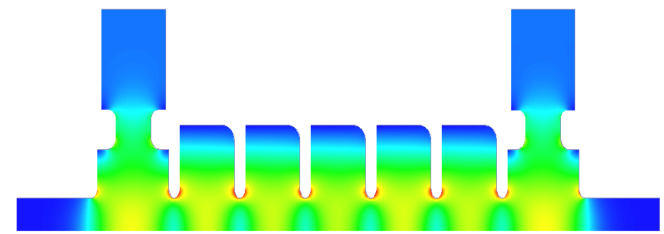

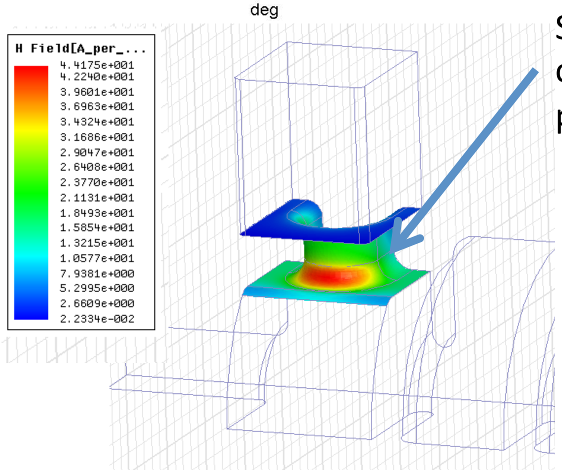

Strongly rounded coupler to reduce the pulsed heating

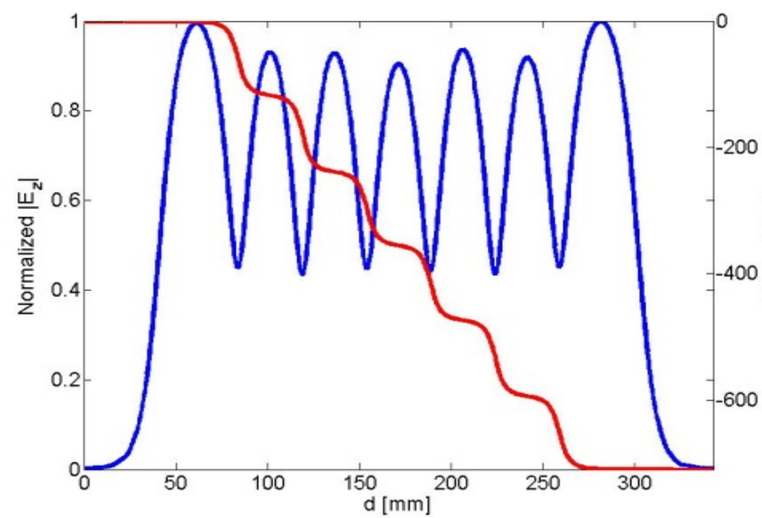

LINAC WITH GASKETS: MECHANICAL DESIGN

The prototype is composed by an input coupler, ten accelerating cells and an out coupler with the final closing cap. The structure will be assembled starting from the input coupler **stacking up one cell after the other**, inserting the gaskets between them and **fixing each part with the previous one by screws**, up to the closing cap. Each cell has eight screw holes disposed at 45° to one another to provide homogeneous force on the gasket when the cells are clamped together. Each parts will be fabricated from cylinders of Oxygen Free High Conductivity (OFHC) copper. The Mechanical design is ready for the machining.

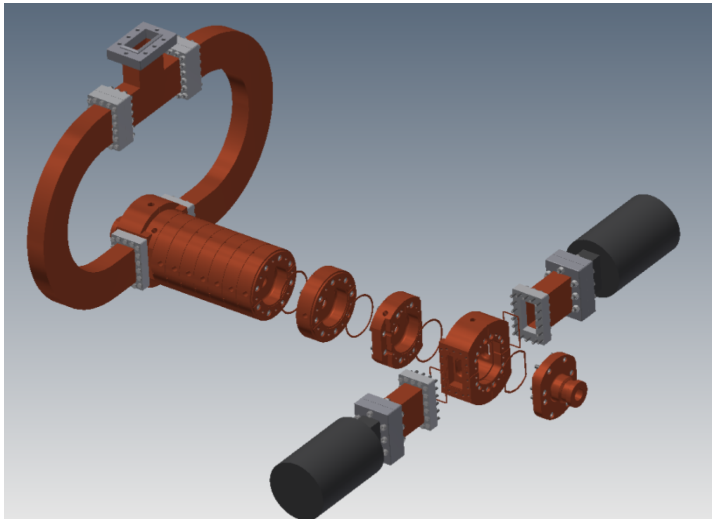

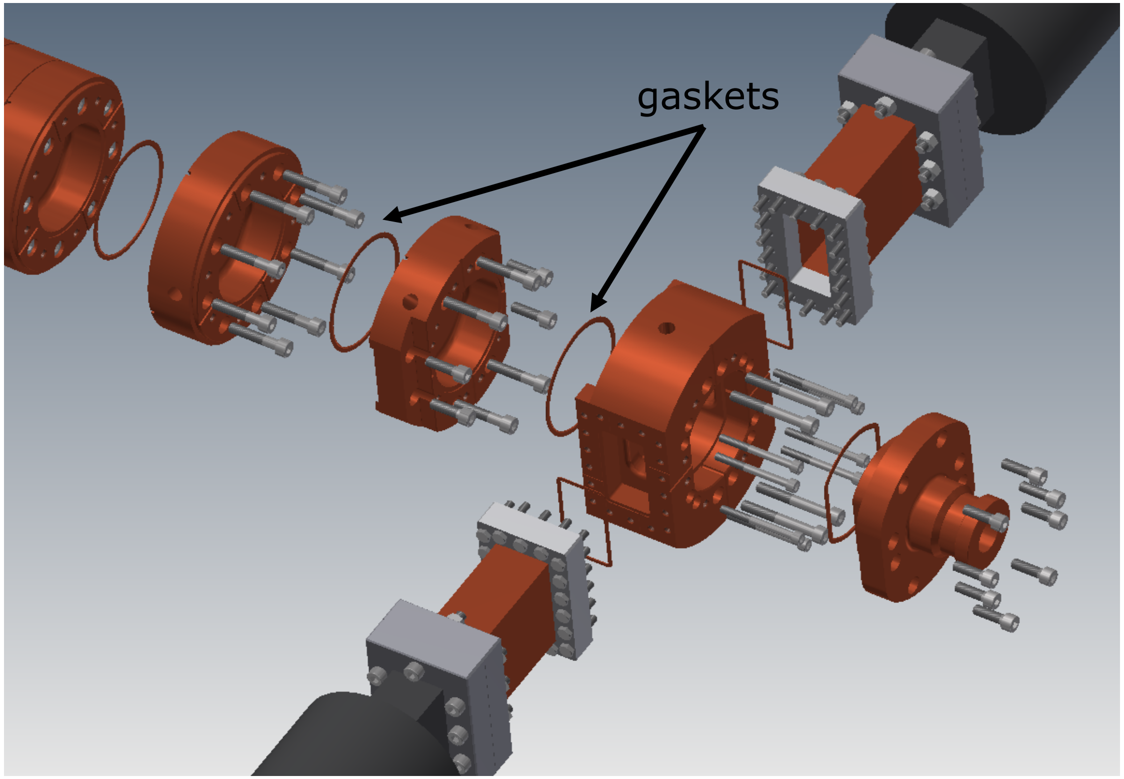

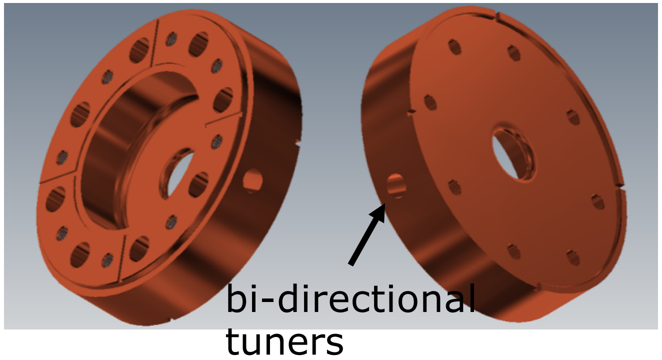

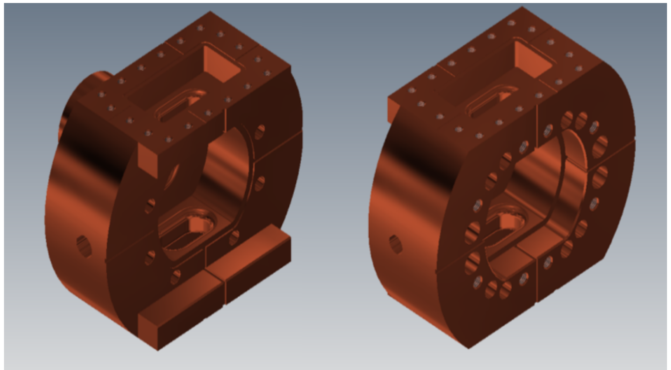

LINAC WITH GASKETS: WORK PROGRAM

The manufacturing will be done at mechanical workshop of the INFN-Roma1

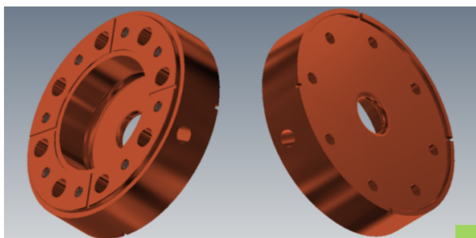

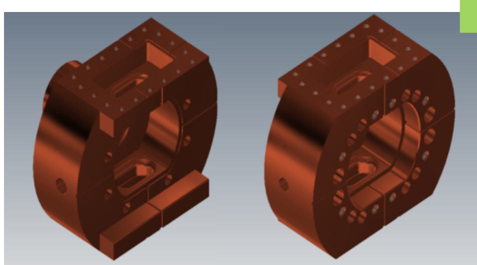

Assembly

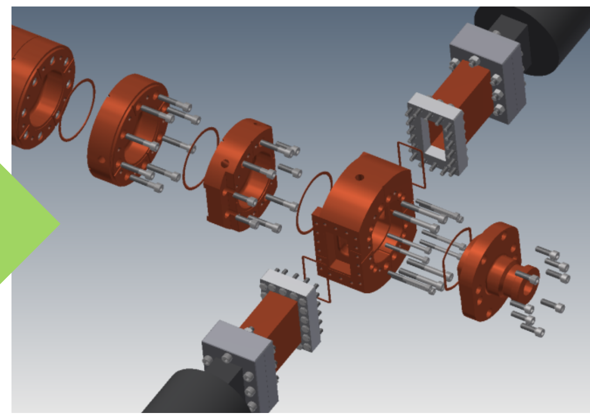

Vacuum leak test, low power measurements and tuning

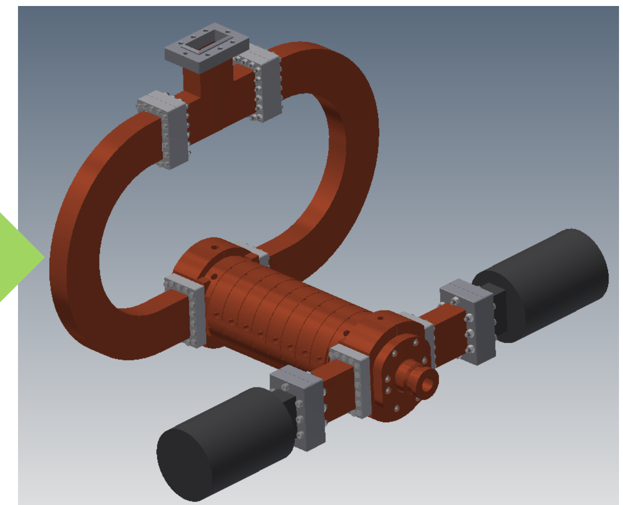

HIGH POWER TEST
TBD

CONCLUSIONS

1. In the ELI-NP GBS, the **high gradient, high repetition rate** and the **multi bunch operation** required a challenging design for the C-band accelerating structures;

2. The **structures** integrate a **damping system** to suppress dipole HOMs, based on waveguides and SiC absorbers. They have been designed, fabricated and tested at the nominal parameters (**33 MV/m, 100 Hz, 820 ns).** The overall electromagnetic and mechanical design has been focalized to guarantee the **required performances and to reduce cost and risk of failure** in the realization process;

3. A **new technique for the realization of RF structures has been** recently developed at LNF-INFN. It **avoids the brazing process**;

4. **Two RF guns** have been designed, fabricated and **successfully high power tested** using this technique: the RF gun for the SPARC-LAB photo-injector and the ELI-NP one. In particular in the ELI-NP one extremely good performances have been reached in a very short conditioning time (100 Hz, 120 MV/m, 1.5 us for Multi Bunch operation);

5. **The new clamping technique using vacuum/RF gaskets could be extended to other RF structures** (S/C/X band) and a LINAC prototype (10 cell) has been design and will be fabricated and tested in the near future.

THANKS TO…

V. Lollo, R. Di Raddo, P. Chimenti, R. Clementi, R. Boni, L. Foggetta, A. Gallo, A. Ghigo, L. Pellegrino, L. Piersanti, F. Cardelli, S. Bini, S. Quaglia, M. Scampati, C. Vaccarezza, S. Pioli, D. Palmer , M. Del Franco, A. Falone, M. Ferrario(LNF-INFN, Frascati)

M. Migliorati, A. Mostacci, S. Tocci, L. Palumbo, M. Magi (Univ. La Sapienza, Rome)

L. Ficcadenti, V. Pettinacci , F. Pellegrino (INFN-ROMA1, Rome)

A. Grudiev, G. De Michele (CERN)

P. Favaron, F. Poletto (LNL, INFN, Padova)

L. Serafini (INFN Milan)

P. Musumeci, E. Pirez, J. Custodio (UCLA, Los Angeles)

COMEB, RI Companies

…AND YOU FOR THE ATTENTION!

BACKUP SLIDES

C-BAND STRUCTURES: BEAM LOADING COMPENSATION

The **main effects of the beam loading is the decrease of the accelerating field gradient** in the structure since the effective field can be assumed as a superposition of the RF field and induced wakefield. The BL can be **compensated with a proper shape of the input RF power**. The monitoring and the tuning of this power shaping is of fundamental importance.

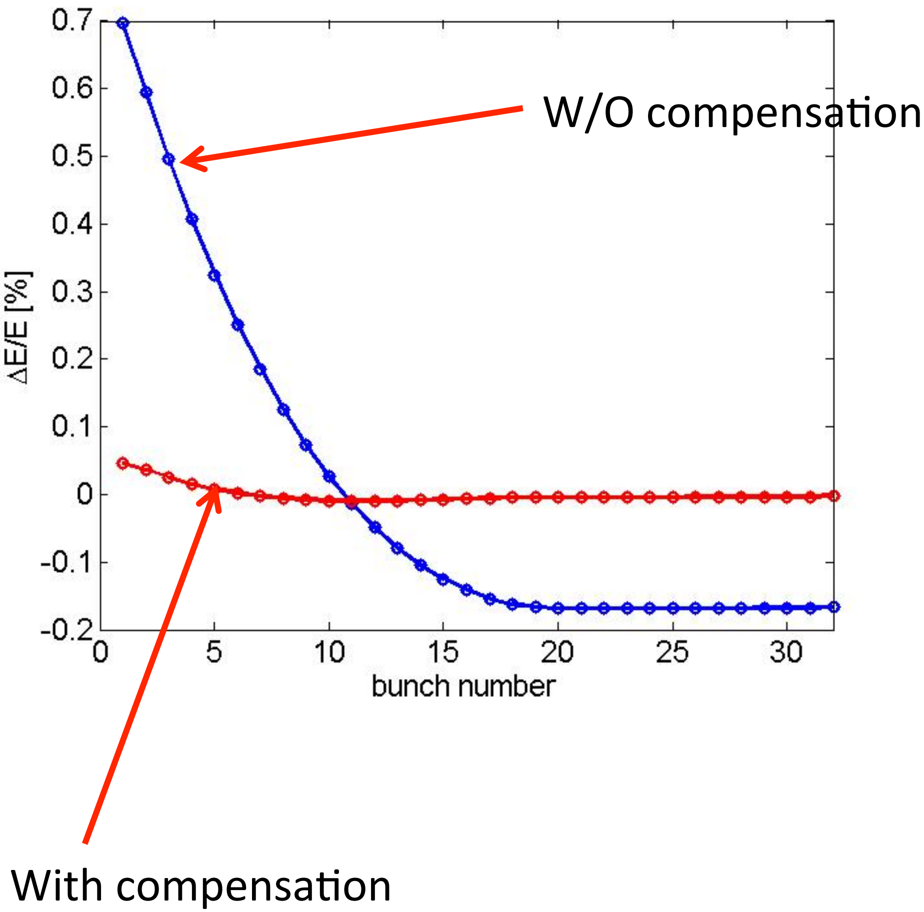

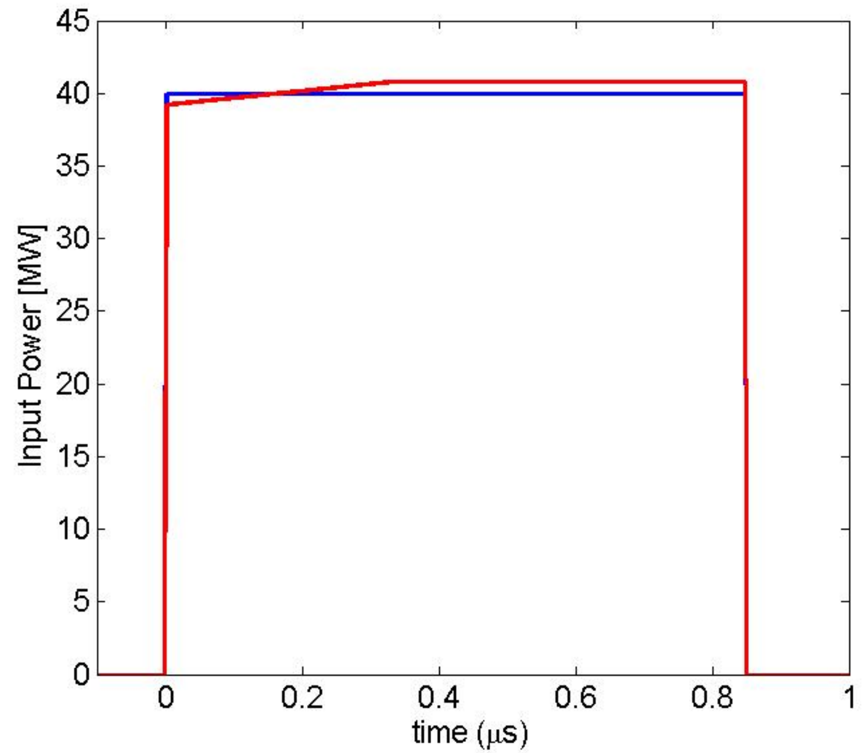

50 MW C-Band RF Unit

Scandinova RF Unit based on Solid State modulator K2-2 adapted for 50MW C-band klystron E37210

50 MW C-Band RF Unit

OPERATIONAL PARAMETERS	
RF Frequency	5712 MHz
RF peak power	50 MW
RF Average power	5 kW
RF driver power	300 W
Operational Voltage range	0 – 370 kV
Operational Current range	0 – 340 A
Modulator Peak power	111 MW
Modulator Average power	32 kW
Repetition rate	1-100 Hz
Beam Pulse length (top)	2 µsec
Top flatness (dV)	<±0.5 %
Amplitude stability	<±0.005 %
Pulse to pulse time jitter	<±4 ns
Rate of Rise	250 – 300 kV/us

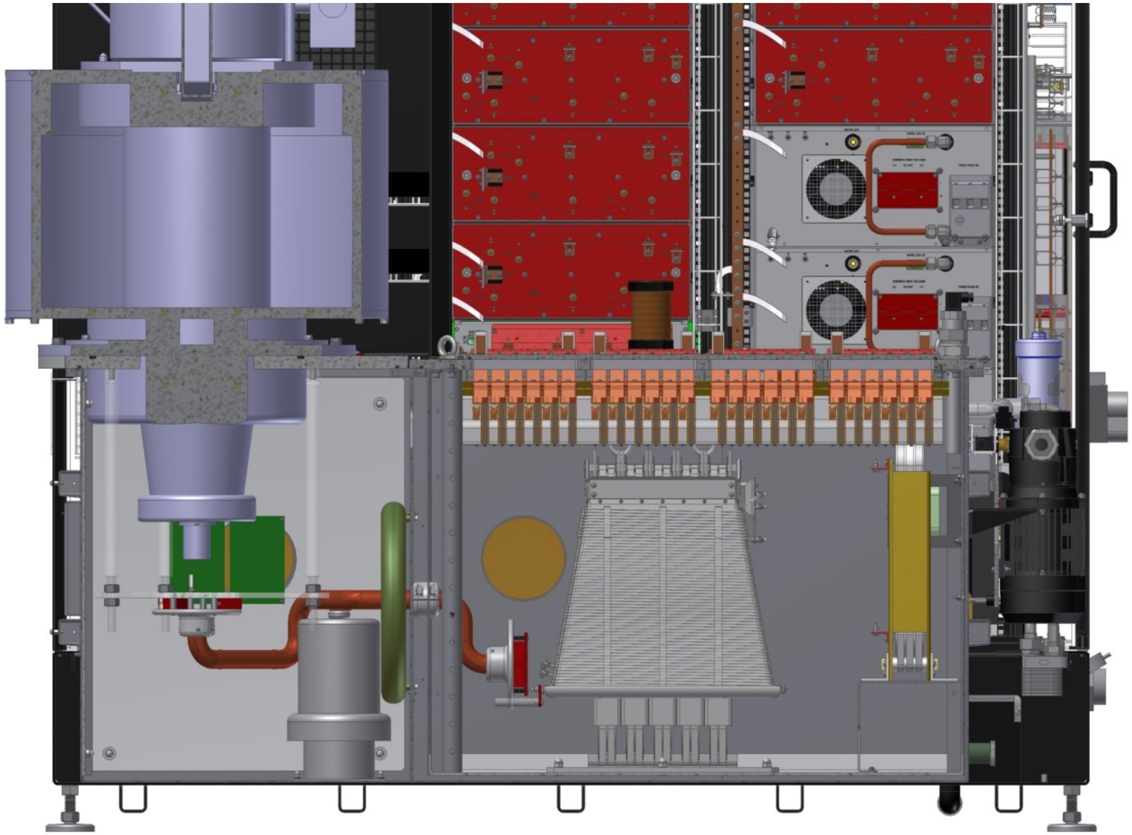

C-band Klystron

Klystron Model	Toshiba E37
Frequency	5712 ±1 MHz
RF output peak power	50 MW (52 Max)
RF pulse repetition rate	100 pps
RF pulse width	1 μsec
Beam voltage	368 kV
Beam current	340 A
Heater Voltage	16 V (24 Max)
Heater Current	18 A (24 Max)
Peak cathode current	325 A
VSWR	1.2:1 (1.5:1 Max)
Radiation level at 1m from the tube	< 100 μSv/h

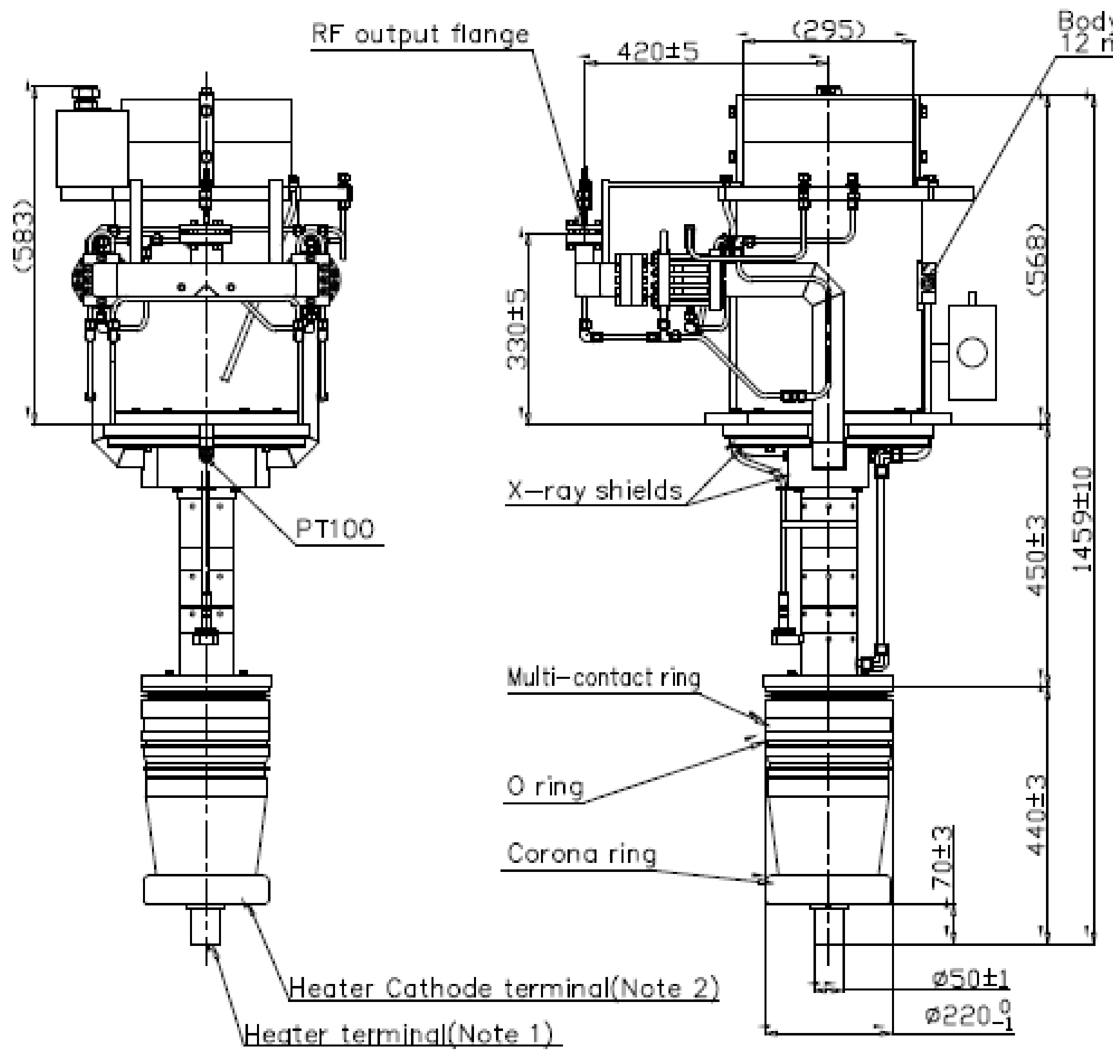

LUMINOSITY PER UNIT BANDWIDTH

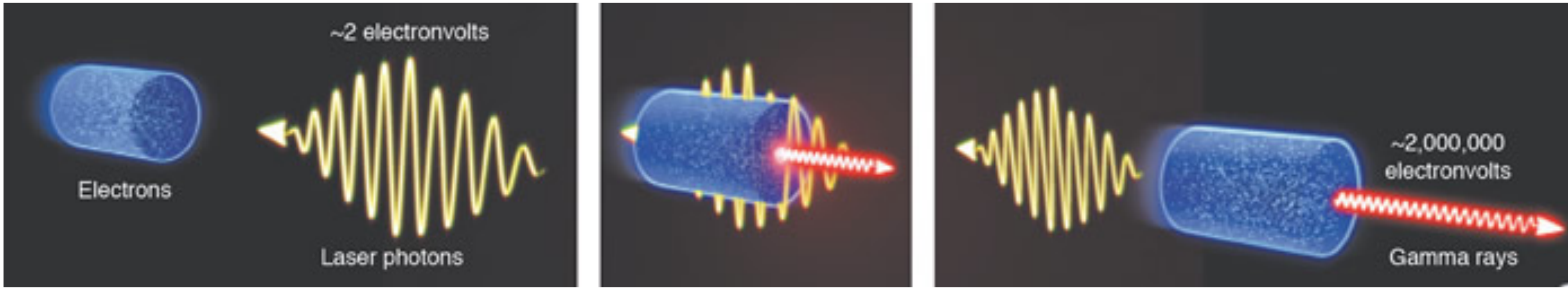

$$\frac{\Delta\nu_\gamma}{\nu_\gamma} \approx \sqrt{(\gamma\theta)^4_{rms} + 4\left(\frac{\Delta\gamma}{\gamma}\right)^2 + \left(\frac{\sqrt{2}\epsilon_n}{\sigma_x}\right)^4 + \left(\frac{\Delta\nu}{\nu}\right)^2 + \left(\frac{M^2\lambda_L}{2\pi w_0}\right)^4 + \left(\frac{a_{0p}^2/3}{1+a_{0p}^2/2}\right)^2}$$

normalised collection angle $\gamma\theta$

electron beam

laser beam

Optimised bandwidth

$$\frac{\Delta\nu_\gamma}{\nu_\gamma} \approx \left(\frac{\sqrt{2}\epsilon_n}{\sigma_x}\right)^2$$

Spectral Luminosity

$$L_\gamma = \frac{L}{\Delta\nu_\gamma} \propto \frac{Q}{\epsilon_n^2}$$

Luminosity

$$L = \frac{N_p N_e}{4\pi\sigma_x^2} f_{rep}$$

Gamma Spectral density ⟷ **Phase space density**

Courtesy of L. Serafini

COMAPARISON WITH OTHER SOURCES

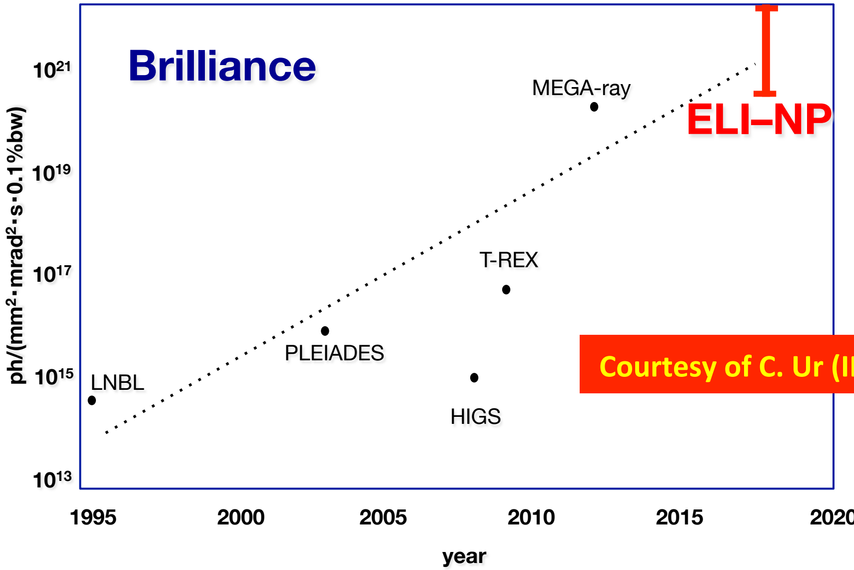

Courtesy of C. Ur (IFIN)

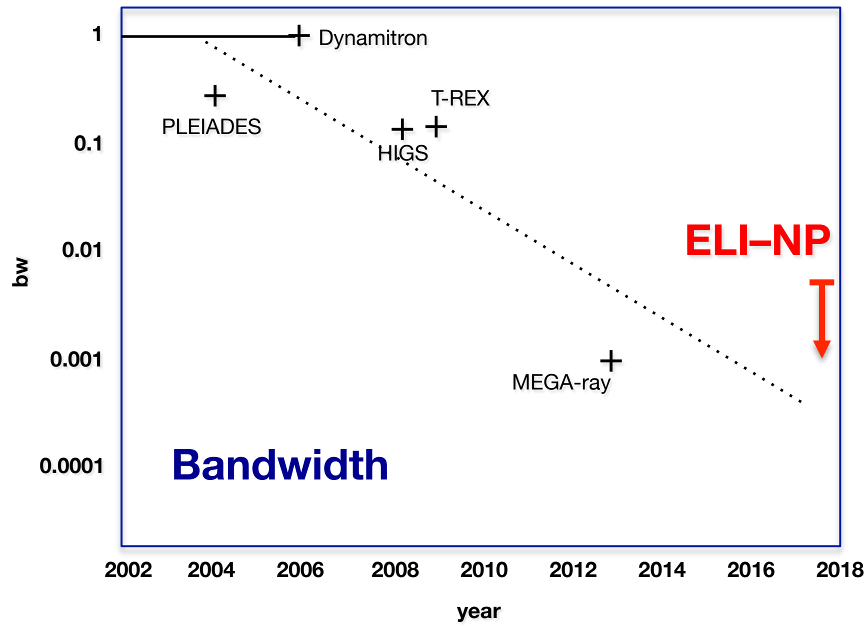

Gamma rays of 1-20MeV with rms bandwidth of 3-5 10^{-3} .

Spectral density:
10^3-10^4 photons/(s eV)

1 order of magnitude improvement in bandwidth

2 order of magnitude improvement in spectral density

Electron beam

$$Q = 250\,pC\ ;\ \varepsilon_n = 4.10^{-7}\,m\cdot rad\ ;\ \Delta\gamma/\gamma = 5\cdot 10^{-4}$$

Laser beam

$$U_L = 400\ \ mJ\ ;\ M^2 = 1.2\ ;\ \frac{\Delta\nu}{\nu} = 5\cdot 10^{-4}$$

by L. Serafini

GAMMA BEAM SYSTEM (GBS) LAYOUT

Courtesy of C. Ur (IFIN)

Low Energy Stage: Gamma rays up to 3.5 MeV

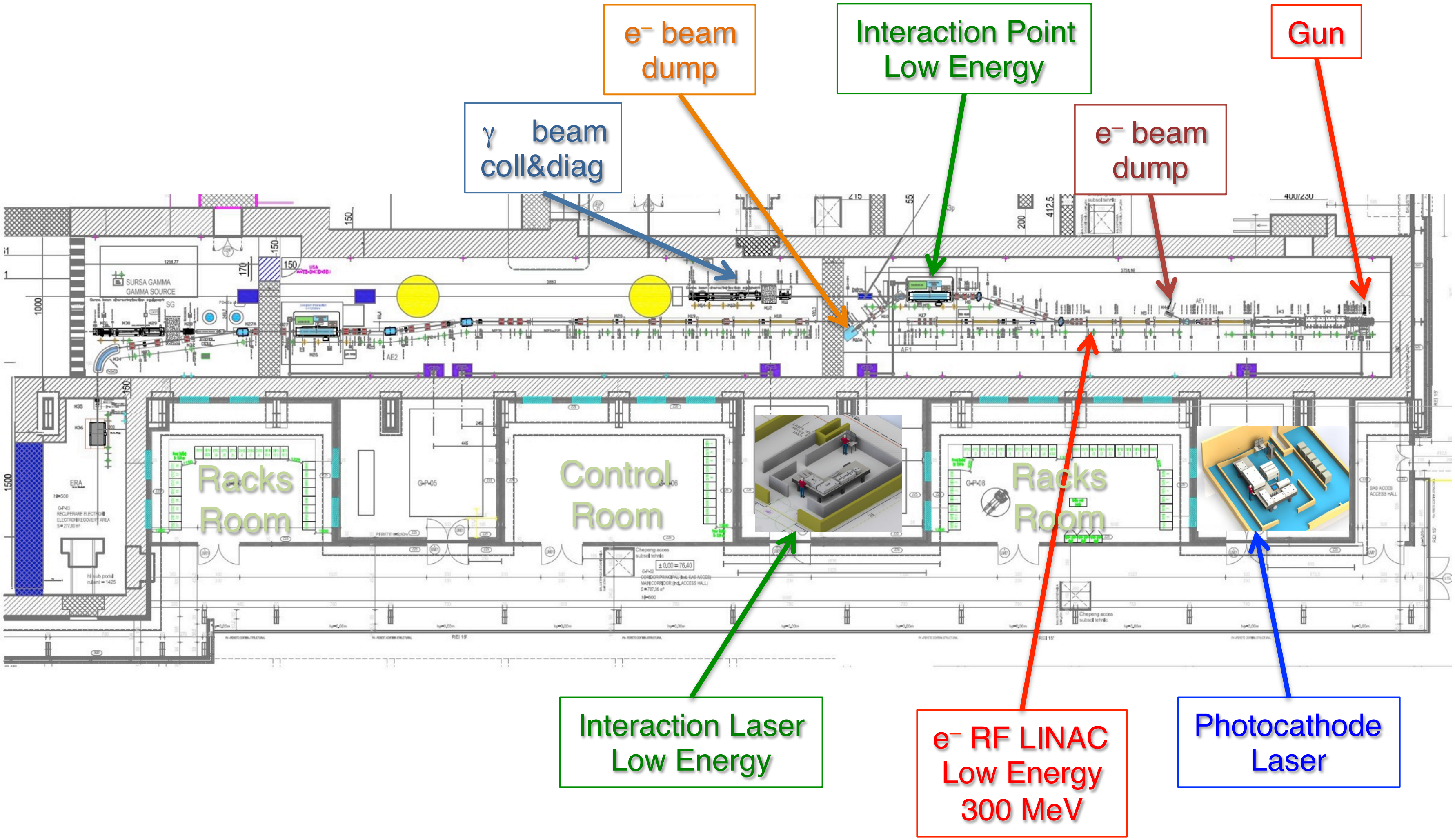

GAMMA BEAM SYSTEM (GBS) LAYOUT

Courtesy of C. Ur (IFIN)

High Energy Stage: Gamma rays up to 19.5 MeV

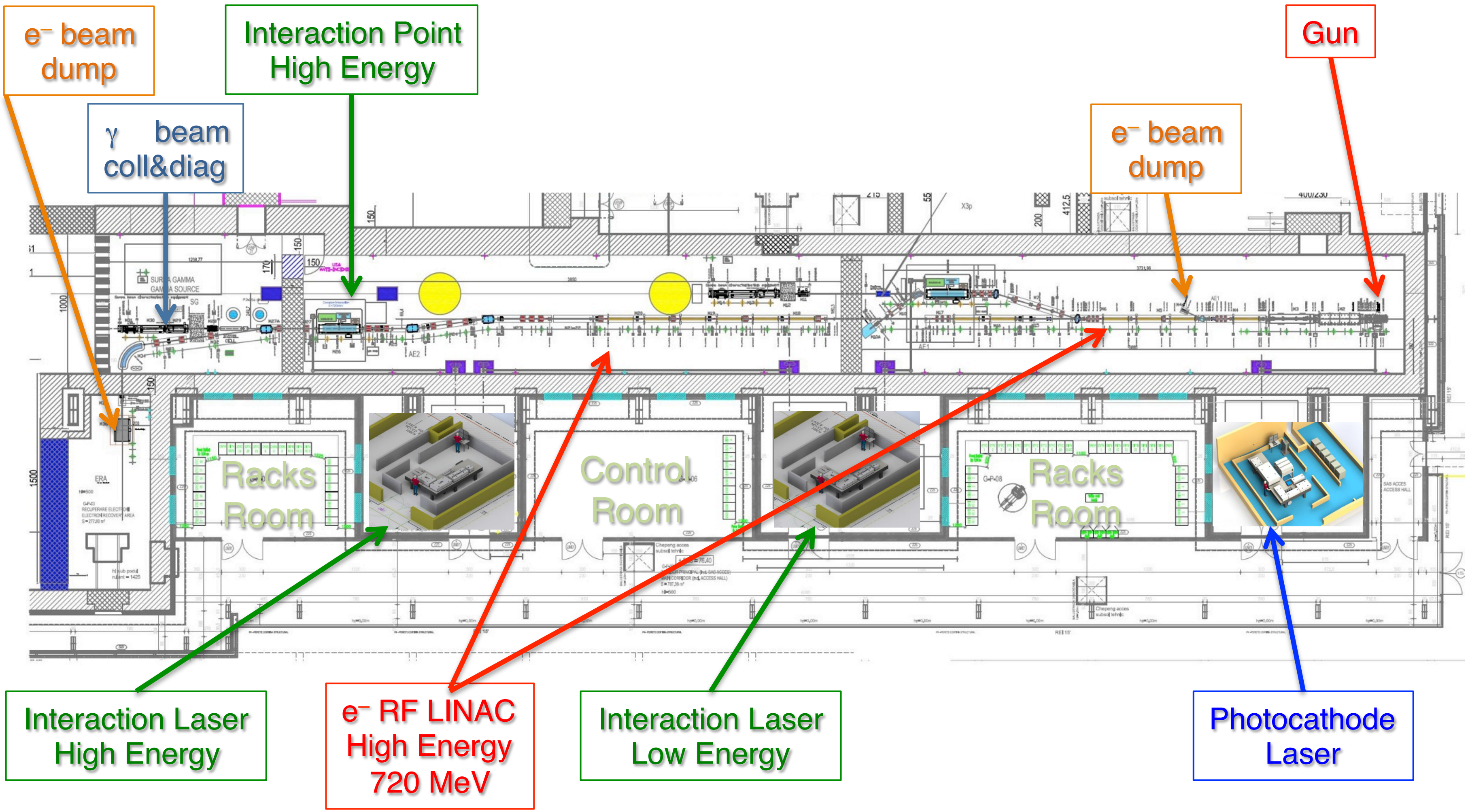

ELECTRON BEAM PARAMETERS @ IP

Energy (MeV)	80 - 720
Bunch charge (pC)	25-400
Bunch length rms (um)	100-400
Norm. emittance in both planes (mm mrad)	0.2-0.6
Bunch energy spread (%)	0.04 – 0.1
Focal Spot size (um)	≥15
Number of bunches in the train	≤32
Bunch separation in the train (ns)	16
Energy variation along the train (%)	0.1
Energy jitter shot to shot (%)	0.1
Emittance dilution due to beam breakup (%)	<10
Time arrival jitter (ps)	<0.5
Pointing jitter (um)	1
RF rep Rate	100 Hz